Ministry of Higher Education and Scientific Research

Abdelhamid Ibn Badis University - Mostaganem

Faculty of Exact Sciences and Computer Science

Department of Physics

Program: Physics

END-OF-STUDY THESIS

For the Obtaining of a Master's Degree in Physics

Option: Materials Physics

Presented by:

CHAMOUMA Amira Kheira

THEME:

The Effective Index Method Applied On Optical Rib Waveguide

Defended on: 11/06/2025

Before the jury composed of:

Mr.Terki Hassaine Mounir	Associate Professor	University of Mostaganem	President
Mr.Belbachir Souheil	Associate Professor	University of Mostaganem	Examiner
Mr.ABBES Charef	Associate Professor	University of Mostaganem	Supervisor

Academic Year 2024-2025

Dedications

"In profound gratitude to the Divine for every moment light and shadow alike”

” Dedicated to the three women who have made my life extraordinary: my strong and loving mother, my wise and caring grandmother (now beyond the veil), and my sweet and funny little sister."

"To my father, my hero, and my friend. Thank you for always being there for me."

“To Sabah,
My compass in chaos, my clarity in confusion “

“And to the lost girl who began this journey, may she recognize herself here.”

Amira.

Acknowledgements

I would like to express my sincere gratitude to all those who have contributed to the successful completion of this work. In particular, I would like to thank:

- **Mr.Terki** and **Mr.Belbachir** for the honor of being part of the examination board.
- **Mr.ABBES** my supervisor for their invaluable guidance, support, and encouragement throughout the project.
- **My classmates** for their helpful suggestions and moral support.

List of figures

Figure N°	Figure title	Page
Figure 1.1	***Military radar***	**6**
Figure 1.2	***Satellite***	**6**
Figure 1.3	***Biosensors: Revolutionizing diverse fields.***	**7**
Figure 1.4	***Fiber-optic.***	**7**
Figure 1.5	***Schematic representation of various channel waveguides.***	**9**
Figure 1.6	***Modes of an asymmetric planar step-index waveguide.***	**15**
Figure 2.1	***Schematic drawing of a symmetric slab waveguide.***	**21**
Figure 2.2	***Schematic drawing of an asymmetric slab waveguide with a core index of n_2***	**27**
Figure 2.3	***Schematic drawing of several two-dimensional waveguides: (a) a rectangular strip of dielectric medium embedded in another dielectric medium of lower index of refraction; (b) ridge waveguide structure; and (c) another ridge structure.***	**34**
Figure 3.1	***3D plot, contour plot and intensity plot of TE_{00} mode.***	**43**
Figure 3.2	***3D plot, contour plot and intensity plot of TE_{01} mode.***	**44**
Figure 3.3	***3D plot, contour plot and intensity plot of TE_{10} mode.***	**44**
Figure 3.4	***Structure of optical rib waveguide.***	**45**
Figure 3.5	***E field distribution where (a) E field in slab region, (b) E field in rib region and (b) E field in lateral region.***	**48-49**
Figure 3.6	***3D plot of field intensity for the second structure***	**49**
Figure 3.7	***The variation of the refractive index vs the rib thickness for TE mode.***	**50**
Figure 3.8	***The variation of the refractive index vs the rib width for TE mode.***	**51**
Figure 3.9	***Comparative curves describing the influence of parameters on confinement.***	**51**
Figure 3.10	***Effective indices vs. rib width and their polarization modification for TM_{00},TE_{00},TM_{01},TE_{01}***	**54**
Figure 3.11	***Comparative curves that show the difference between lateral and total confinements for fundamental mode***	**55**
Figure 3.12	***Comparative curves that show present the lateral field intensity in the rib waveguide for***	**55**

	TE and TM polarizations for two different width value.	
Figure 3.13	***Effective indices vs. operating wavelength and their polarization modification for TM_{00},TE_{00},TM_{01},TE_{01}.***	**56**

List of tables

Table N°	**Table title**	***Page***
Table 1.1	***Classification by Dimensionality of Confinement.***	***8***
Table 1.2	***Classification according to geometry.***	***9***
Table 1.3	***Comparative analysis of computational methods in photonics: types, domains and characteristics.***	***18***
Table 3.1	***Parameters for an optical rib waveguide structure.***	***44***
Table 3.2	***Effective indices calculated using the effective index method (EIM) for the TE_{00} mode.***	***46***
Table 3.3	***Effective indices calculated using the effective index method for the TM_{00} mode.***	***46***
Table 3.4	***Optical and Geometrical structure parameters of GaAs and GeSi rib wave guides.***	***47***
Table 3.5	***Comparison of Effective indices values for GaAs Geometries Using Different Methods.***	***47***
Table 3.6	***Optical and Geometrical structure parameters of GaAs and GeSi rib wave guides***	***48***
Table3.7	***Parameters for an optical rib waveguide structure.***	***50***
Table 3.8	***Parameters for an optical rib waveguide structure for TE mode.***	***53***
Table 3.9	***Parameters for an optical rib waveguide structure for TM mode.***	***53***

List of abbreviations

Abbreviation	*Definition*
BPM	***Beam Propagation Method (numerical technique for waveguide analysis)***
CMOS	***Complementary Metal-Oxide-Semiconductor (fabrication technology)***
EIM	***Effective Index Method (semi-analytical waveguide modeling approach)***
EME	***Eigenmode Expansion (frequency-domain numerical method)***
FDTD	***Finite-Difference Time-Domain (time-domain numerical method)***
FEM	***Finite Element Method (frequency-domain numerical method)***
FFM	***Finite Fourier Method (validation technique)***
GaAs	***Gallium Arsenide (semiconductor material)***
GaAlAs	***Gallium Aluminum Arsenide (semiconductor material)***
HOC-FDM	***High-Order Compact Finite-Difference Method (validation technique)***
InP	***Indium Phosphide (semiconductor material)***
IPC-E	***Isophorone diisocyanate-based Polyphosphonate Ester (polymer material)***
$LiNbO_3$	***Lithium Niobate (electro-optic material)***
MMF	***Multi-Mode Fiber (waveguide supporting multiple propagation modes)***
MoL	***Method of Lines (analytical technique)***
NOA72	***Norland Optical Adhesive 72 (UV-curable epoxy)***
PCF	***Photonic Crystal Fiber (3D waveguide type)***
PIC	***Photonic Integrated Circuit (application domain)***
PLCs	***Planar Lightwave Circuits (application domain)***
PMMA	***Polymethyl Methacrylate (polymer material)***
PSU	***Polysulfone (polymer matrix material)***
PWE	***Plane Wave Expansion (frequency-domain numerical method)***
QKD	***Quantum Key Distribution (quantum photonics application)***
RI	***Refractive Index (material property)***
RIE	***Reactive Ion Etching (fabrication technique)***
DRIE	***Deep Reactive Ion Etching (fabrication technique)***
SHG	***Second-Harmonic Generation (nonlinear optical phenomenon)***
Si_3N_4	***Silicon Nitride (waveguide material)***
SMF	***Single-Mode Fiber (waveguide supporting single propagation mode)***
SOI	***Silicon-on-Insulator (material platform)***
SSM	***Split-Step Method (time-domain numerical method)***
SU-8	***Epoxy-based negative photoresist (polymer material)***
TE	***Transverse Electric (mode polarization)***
TM	***Transverse Magnetic (mode polarization)***
TMM	***Transfer Matrix Method (frequency-domain numerical method)***
VPM	***Variational Perturbation Method (validation technique)***
WDM	***Wavelength-Division Multiplexing (telecom application)***

Abstract

The unprecedented advancement of optical telecommunications and integrated optics relies critically on optical rib waveguides as foundational enabling structures

This study presents a comprehensive theoretical analysis of rib waveguides using the Effective Index Method (EIM). We systematically quantify the influence of structural parameters (rib width W, height H, slab thickness) and refractive index contrast on modal characteristics, including propagation constants (β), confinement factors (Γ), and single-mode operation thresholds.

While EIM proves efficient for rapid integrated photonic circuit design, its fidelity diminishes for subwavelength structures, nanostructures, or waveguides with significant sidewall roughness and radiation losses. This work establishes quantitative guidelines for optimizing light confinement and polarization resilience, extending toward quantum photonic applications and topological waveguides.

Keywords: Rib waveguide, Effective Index Method (EIM), Silicon-on-Insulator (SOI), modal analysis, confinement factor, propagation constant, single-mode operation, refractive index contrast, modal dispersion, radiation losses, sidewall roughness, integrated photonics, quantum photonics.

ملخص

يعتمد التقدم غير المسبوق في الاتصالات البصرية والبصريات المتكاملة بشكل حاسم على الموجات الدليلية الضوئية ذات الهيكل الضلعي كعناصر تمكينية أساسية.
تقدم هذه الدراسة تحليلاً نظرياً شاملاً للموجات الدليلية الضلعية باستخدام طريقة المؤشر الفعال نقوم بتحديد كمي منهجي لتأثير المعاملات الهيكلية (عرض الضلع ، الارتفاع ، سماكة الطبقة التحتية) والتباين في معامل الانكسار على الخصائص النمطية، بما في ذلك ثوابت الانتشار ، عوامل الحصر ، وعتبات التشغيل أحادي النمط.
بينما تثبت طريقة EIM كفاءتها في التصميم السريع للدوائر الضوئية المتكاملة، فإن دقتها تتناقص في الهياكل دون الطول الموجي، والهياكل النانوية، أو الموجات الدليلية ذات خشونة الجوانب والفقد الإشعاعي الكبيرين.
يضع هذا العمل إرشادات كمية لتحسين حصر الضوء ومقاومة الاستقطاب، ممتداً نحو تطبيقات الفوتونيات الكمية والموجات الدليلية الطوبولوجية.

الكلمات المفتاحية:

الموجة الدليلية الضلعية، طريقة المؤشر الفعال ، السيليكون على العازل ، التحليل النمطي، عامل الحصر، ثابت الانتشار، التشغيل أحادي النمط، تباين معامل الانكسار، التشتت النمطي، الفقد الإشعاعي، خشونة الجوانب، الفوتونيات المتكاملة، الفوتونيات

Résumé

Les progrès sans précédent des télécommunications optiques et de l'optique intégrée reposent de façon cruciale sur les guides d'onde optiques à nervure en tant que structures fondamentales. Cette étude présente une analyse théorique complète des guides d'onde à nervure en utilisant la Méthode de l'Indice Effectif (EIM).Nous quantifions systématiquement l'influence des paramètres structurels (largeur de la nervure W, hauteur H, épaisseur de la couche inférieure) et du contraste d'indice de réfraction sur les caractéristiques modales, incluant les constantes de propagation (β), les facteurs de confinement (Γ), et les seuils de fonctionnement monomode.
Bien que l'EIM s'avère efficace pour la conception rapide de circuits photoniques intégrés, sa sa fiabilité diminue pour les structures sub-longueur d'onde, les nanostructures ou les guides d'onde présentant une rugosité latérale et des pertes par rayonnement significatives. Ce travail établit des directives quantitatives pour optimiser le confinement lumineux et la résilience à la polarisation, en s'étendant vers les applications photoniques quantiques et les guides d'onde topologiques.

Mots-clés:

Guide d'onde à nervure, Méthode de l'Indice Effectif (EIM), Silicium sur Isolant (SOI), analyse modale, facteur de confinement, constante de propagation, fonctionnement monomode, contraste d'indice de réfraction, dispersion modale, pertes par rayonnement, rugosité des parois latérales, photonique intégrée, photonique quantique.

Table of contents

General Introduction 1

Chapter 01: Generalities about waveguides and photonics. 4

Introduction 4

1.1.Guiding Light: A breif History of electromagnetics: 4

1.2.Definition of a waveguide: 5

1.3.Non-optical waveguides : 6

1.3.1.Characteristics of Non-Optical Waveguides: 6

1.4. Optical waveguides: 6

1.4.1. Characteristics of Optical Waveguides: 7

1.5. Types and classifications of waveguides: 7

1.5.1. Classification by dimensionality of confinement 8

1.5.2.Classification according to geometry 9

1.6. A brief overview on planar waveguides,2D waveguides and 3D waveguides 10

1.6.1. Planar Waveguides (1D Optical Confinement) 10

1.6.2. 2D Waveguides (Channel/Rib Structures) 10

1.6.3. 3D Waveguides (Optical Fibers & Photonic Crystal Structures) 10

1.7. Materials for optical waveguide fabrication: 11

1.7.1. Core and Cladding Materials 11

1.7.2. Substrates 11

1.8. Fabrication techniques and applications: 12

1.9. Understanding Light: Rays, Waves, and Wave fronts 12

1.10. Guided modes : 13

1.11. Definition of Photonics : 15

1.12. Core Principles of Photonics : 16

Light Propagation and Maxwell's Equations 16

Waveguide Theory 16

Light-Matter Interaction 16

Quantum Nature of Light 16

1.13. Methods and Approximations for wveguide analysis: 17

1.13.1. Time-domain methods: 17

1.13.2. Frequency-domain methods 17

1.13.3. Effective Index Method (EIM)"semi-analytical hybrid method" 18

Conclusion 19
Chapter 02: Planar Waveguide Analysis (Effective Index Method and Modes Characterizations). 20
Introduction 20
3.1. Maxwell equations 20
2.2. Planar optical waveguides: 21
2.2.1. Slab waveguides 21
2.2.3. Unified theory of waveguides 22
2.2.4. Guided TE modes 23
2.2.5. Guided TM modes 25
2.3. TE and TM confined modes in asymmetric slab waveguide: 26
2.3.1. Guided TE modes 27
2.3.2. Guided TM modes 29
3.3.3. Mode Confinement Factor 32
2.4. Effective index theory 33
Conclusion 36
Chapter 03: Results and Discussions. 37
Introduction 37
3.1.Rib waveguide 37
3.1.1. Structure of rib Waveguides 37
3.1.2. Importance of Rib Waveguides 37
3.1.3. Applications 38
3.1.4. Advantages of Rib Waveguides 38
3.1.5. Disadvantages and Challenges 38
3.2. The contrast effect: 39
3.3. Classification of waveguide by mode structure: 39
3.3.1. Single-mode waveguide: 39
3.3.2. Multi-mode waveguide: 39
3.4. Software Maple 39
3.5.The advantages and limitations of the Effective Index Method (EIM) 40
3.5.1. Advantages of EIM 40
3.5.2. Limitations of EIM 41
3.6.Validation of program: 43
3.6.1. Structure 45
3.7. Contrast effect 48

3.8. Optimisation of a single-mode rectangular rib waveguide 50
3.9. Analysis of optical rib waveguides based organic/polymer materials. 52
3.9.1. Optimizing Rib Waveguide Width 52
3.9.2. Spectral optimization 56
Conclusion 57
General conclusion 58
Future Perspective 59
Quantum-Enhanced Photonic Integration 59
Optical Neural Acceleration via Programmable Waveguides 59
Bibliography 60

The effective index method applied on optical rib waveguide.

General Introduction

Optical waveguides form the backbone of modern photonic systems, playing a critical role in the transmission, manipulation, and processing of optical signals. From their early conceptualization to their widespread adoption in integrated photonic circuits, waveguides have evolved into essential components across numerous technological fields, including telecommunications, sensing, medical imaging, and quantum information processing.

The concept of guiding light dates back to the 19th century, but practical implementations emerged in the mid-20th century, particularly with the invention of optical fibers in the 1960s. This breakthrough enabled the development of long-distance optical communication, setting the stage for rapid progress in fiber optics and, later, in integrated optics. As optical systems grew more complex and the demand for miniaturization increased, researchers began to explore alternatives to fiber-based systems, leading to the rise of planar waveguide technologies.

In general terms, an optical waveguide is a physical structure that confines and directs electromagnetic waves along a desired path. It typically consists of a core region with a higher refractive index than its surrounding cladding, allowing light to be confined through total internal reflection. The specific geometry and material composition of the waveguide determine its guiding properties, modal behavior, and application suitability.

A wide variety of waveguide geometries have been proposed and developed, each offering distinct advantages for different applications. The most common configurations include slab waveguides (1D confinement), channel waveguides (2D confinement), strip and ridge waveguides, and photonic crystal waveguides. Among these, the rib waveguide stands out as a practical compromise between strong confinement and ease of fabrication.

A rib waveguide typically consists of a raised rectangular ridge or strip etched into a slab of guiding material. Unlike fully etched channel waveguides, the rib structure leaves a portion of the slab layer intact, which provides improved mode confinement in the vertical direction while allowing for relatively simple fabrication. This design supports single-mode propagation under appropriate geometric conditions and exhibits reduced sensitivity to sidewall roughness and fabrication imperfections.

Rib waveguides are extensively used in silicon photonics, a field that exploits the optical properties of silicon to build high-performance photonic devices using standard semiconductor

manufacturing techniques. The dominant material platform in this field is Silicon-on-Insulator (SOI), which consists of a thin silicon device layer separated from a silicon substrate by a buried oxide (SiO_2) layer. The high refractive index contrast between silicon ($n \approx 3.45$ at 1550 nm) and silica ($n \approx 1.44$) enables tight mode confinement and compact device footprints, making SOI-based rib waveguides highly suitable for dense photonic integration.

Besides silicon, other materials used for rib waveguides include gallium arsenide (GaAs), indium phosphide (InP), silicon nitride (Si_3N_4), lithium niobate ($LiNbO_3$), and polymer-based materials. The choice of material depends on several factors, such as operating wavelength, optical loss, nonlinear properties, thermal stability, and compatibility with electronic components.

To understand and optimize the performance of rib waveguides, several analytical and numerical modeling techniques are employed. These include rigorous methods like the Finite-Difference Time-Domain (FDTD) method, the Finite Element Method (FEM), the Beam Propagation Method (BPM), and the Method of Lines (MoL). While these methods offer high accuracy, they can be computationally intensive, especially for large parameter sweeps or complex geometries.

As an alternative, semi-analytical techniques provide faster solutions with acceptable accuracy, particularly during the initial design phase. One of the most widely used semi-analytical methods is the Effective Index Method (EIM). This method simplifies the analysis of complex two-dimensional (or three-dimensional) waveguide structures by decomposing them into a sequence of one-dimensional problems.

The EIM is particularly well-suited for rib waveguides due to the quasi-separable nature of their refractive index profile. The method involves two main steps: first, solving a one-dimensional slab waveguide problem in the vertical direction to obtain an effective refractive index; second, treating this effective index as a virtual refractive index for the lateral confinement problem. The resulting effective indices closely approximate the propagation constants of the actual guided modes, especially in structures with moderate index contrast and symmetric geometries.

Despite its approximate nature, the EIM provides valuable insights into the modal properties, such as cutoff conditions, mode field distribution, and confinement factors. It is also instrumental in identifying the single-mode regime and in predicting how changes in geometry

(e.g., rib height, width, and slab thickness) influence the effective index and guiding characteristics.

This master's thesis is devoted to the theoretical investigation of rib waveguides using the Effective Index Method. The primary aim is to analyze the influence of structural and material parameters on the modal behavior and confinement of light within the waveguide. The study focuses on determining the effective index of the fundamental mode as a function of rib dimensions, core height, and refractive index contrast, with a particular emphasis on the SOI platform due to its relevance in integrated photonics.

Through a systematic exploration of different configurations, the thesis highlights the advantages and limitations of the EIM in practical design scenarios. The results obtained are compared to known analytical and numerical models to validate the accuracy and applicability of the method. Additionally, the findings contribute to the understanding of design trade-offs in rib waveguides, such as between confinement efficiency and fabrication tolerance.

Ultimately, this work seeks to provide a solid theoretical foundation for the use of rib waveguides in integrated photonic systems, demonstrating how the Effective Index Method can serve as a rapid and reliable design tool for next-generation optical components.

Chapter one builds the foundational knowledge needed to understand waveguides and photonics. It mainly includes waveguide types, classification by geometry and confinement and a comparative look at analytical and numerical modeling methods, leading into the Effective Index Method (EIM) as a compromise between complexity and practicality.

Chapter two provides the theoretical backbone for waveguide analysis. It deals in detail with slab waveguides, presents, and explains in depth the Effective Index Method (EIM).

In chapter three, we apply the EIM to rib waveguides and discusses practical results and design implications. We present optimization studies, where we examine contrast effects and mode classification (single-mode and multi-mode). The influence of rib width and core thickness is examined and spectral optimization and confinement trade-offs are discussed.

Chapter 01: Generalities about waveguides and photonics.

1.1.Introduction

This chapter establishes the foundational principles of guided-wave photonics, tracing the historical unification of electromagnetics and optics through Maxwell's equations. We define waveguide architectures across electromagnetic spectra, classify confinement mechanisms (1D–3D), and characterize light-guiding phenomena through ray-wave duality. Core photonic principles from material selection to modal analysis are contextualized with emerging quantum applications. The chapter concludes with a critical comparison of computational methods, setting the stage for the Effective Index Method's specialized role in waveguide analysis.

1.2. Guiding light: A brief history of electromagnetics:

Electricity and magnetism have been known to humans for a long time. Also, the physical properties of light has been known. But electricity and magnetism, now termed electromagnetics in the modern world, has been thought to be governed by different physical laws as opposed to optics. This is understandable as the physics of electricity and magnetism is quite different of the physics of optics as they were known to humans. For example, lodestones (Fe_3O_4) was known to the ancient Greek and Chinese around 600 BC to 400 BC. Compass was used in China since 200 BC. Static electricity was reported by the Greek as early as 400 BC. But these curiosities did not make an impact until the age of telegraphy. The coming about of telegraphy was due to the invention of the voltaic cell or the galvanic cell in the late 1700s, by Luigi Galvani and Alesandro Volta. It was soon discovered that two pieces of wire, connected to a voltaic cell, can be used to transmit information. So by the early 1800s this possibility had spurred the development of telegraphy. Both André-Marie Ampére (1823) and Michael Faraday (1838) did experiments to better understand the properties of electricity and magnetism. And hence, Amperes law and Faraday law are named after them. Kirchhoff’s voltage and current laws were also developed in 1845 to help better understand telegraphy. Despite these laws, the technology of telegraphy was poorly understood. It was not known as to why the telegraphy signal was distorted. Ideally, the signal should be a digital signal switching between ones and zeros, but the digital signal lost its shape rapidly along a telegraphy line.It was not until 1865 that James Clerk Maxwell put in the missing term in Amperes law, the term that involves

displacement current, only then the mathematical theory for electricity and magnetism was complete. Amperes law is now known as generalized Amperes law. The complete set of equations are now named Maxwell's equations in honor of James Clerk Maxwell. The rousing success of Maxwell's theory was that it predicted wave phenomena, as they have been observed along telegraphy lines. Heinrich Hertz in 1888 did experiment to proof that electromagnetic field can propagate through space across a room. Moreover, from experimental measurement of the permittivity and permeability of matter, it was decided that electromagnetic wave moves at a tremendous speed. But the velocity of light has been known for a long while from astronomical observations. The observation of interference phenomena in light has been known as well. When these pieces of information were pieced together, it was decided that electricity and magnetism, and optics, are actually governed by the same physical law or Maxwell's equations. And optics and electromagnetics are united into one field.

The late 20th century witnessed the burgeoning fields of nano-fabrication, the delicate art of single-photon measurement, and the intertwined disciplines of quantum optics and nano-optics. Furthermore, the conceptual revolution of quantum information, underscored by Bell's theorem, has laid the groundwork for the anticipated emergence of quantum electromagnetics and optics, hinting at future technological landscapes yet to be fully realized. This intricate tapestry of scientific inquiry and technological innovation underscores humanity's relentless pursuit of knowledge and its power to reshape our understanding of the universe. [1]

1.3. Definition of a waveguide:

Waveguides represent a specialized class of transmission lines designed for efficient propagation of electromagnetic waves through confined structures. These devices fundamentally guide wave energy along their longitudinal axis while restricting spatial expansion of the field. The most common implementation involves hollow metallic conduits, typically rectangular or circular in cross-section, which constrain wave propagation through boundary conditions established by their conducting walls. These structures exhibit distinct advantages over conventional transmission lines, particularly at microwave and millimeter-wave frequencies, where their low-loss characteristics and power handling capabilities become essential. [2]

1.4. Non-optical waveguides :

Structures that guide non-optical electromagnetic waves, such as microwaves, radio waves, or terahertz radiation, often using metallic or dielectric boundaries.Metallic waveguides enforce boundary conditions via conducting walls, supporting TE/TM modes.Ohmic losses dominate in metallic waveguides, scaling with surface roughness and conductivity. Rectangular waveguides are standard in high-power radar systems due to low dispersion. [3]

1.4.1 .Characteristics of non-optical waveguides

- **Material**: Metals (e.g., copper, aluminum) or low-loss dielectrics (e.g., alumina).
- **Frequency Range**: kHz to THz (non-optical spectrum).
- **Loss Mechanisms**: Ohmic losses (metallic), dielectric losses.
- **Examples**:
  - **Metallic rectangular waveguides**: Hollow metal pipes for microwaves.
  - **Coaxial cables**: Central conductor surrounded by dielectric and shield.
  - **Dielectric RF waveguides**: Polymer-based guides for millimeter waves. [4]
    - **Applications**: Radar systems, satellite communications, microwave circuits.

Figure 1.1 : Military radar.

Figure 1.2: Satellite.

1.5. Optical waveguides:

Structures designed to confine and guide light (visible, infrared, or ultraviolet wavelengths) using principles like total internal reflection or photonic bandgap effects "Optical waveguides rely on refractive index contrast for light confinement. [5]

1.5.1. Characteristics of Optical Waveguide

- **Material**: Dielectric materials (e.g., silica glass, silicon, polymers…).

- **Frequency Range**: ~100 THz to 1000 THz (optical spectrum).
- **Loss Mechanisms**: Absorption, scattering, bending losses.
- **Examples**:
  - **Optical fibers**: Core-clad structure for long-distance transmission.
  - **Planar waveguides**: Thin-film layers for on-chip photonics.
  - **Photonic crystal waveguides**: Periodic structures for light control.
- **Applications**: Fiber-optic communications, integrated photonics, biosensors. [6]

Figure 1.3: Biosensors: Revolutionizing diverse fields.

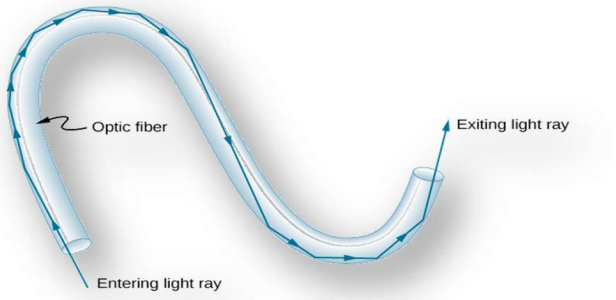

Figure 1.4:Fiber-optic.

1.6. Types and classifications of waveguides:

Waveguide structures are spatially inhomogeneous structures which can guide waves. For light propagating in a waveguide, the self-consistency condition for a mode is more strict than for free-space modes: the shape of the complex amplitude profile in the transverse dimensions must remain exactly constant: any re-scaling is not allowed, only an overall phase change and a loss or gain of total optical power, which are both described by the propagation constant.

Optical waveguides can be classified according to their geometry, mode structure, refractive index (RI) distribution, and material. A dielectric optical waveguide comprises a longitudinally extended high-index medium called the Core, which is transversely surrounded by a low-index medium, called the Cladding.

1.6.1. Classification by dimensionality of confinement

It is famous *that* waveguides are first classified by their confinement dimensionality (planar, channel, or volumetric), then by cross-sectional geometry so let's start with *classification by dimensionality of confinement;* A guided optical wave propagates in the waveguide along the longitudinal direction. The characteristics of a waveguide are determined by the transverse profile of its dielectric constant, which is independent of the z coordinate. For a waveguide made of optically isotropic media, the waveguide can be characterized merely with a single spatially dependent transverse profile of the index of refraction.Broadly, the waveguides can be classified as: [7]

Type	Confinement	Structure Examples	Key Properties	Applications
Planar (Slab)	1D (Vertical)	Layered thin films (e.g., $SiO_2/Si/SiO_2$)	• Vertical confinement only • Unconfined laterally • Low loss	Lasers, sensors, electro-optic modulators
Channel	2D (Vertical + Lateral)	Rib, strip, slot, buried waveguides	• Full lateral + vertical control • Tailorable mode profiles	Integrated photonic circuits (PICs), splitters
3D Waveguides	3D (Full volumetric)	Woodpile photonic crystals, microsphere resonators	• Confinement in all directions • Ultra-high Q-factors ($>10^6$) • Complex fabrication	Quantum light sources, ultra-sensitive biosensors

Table 1.1: Classification by Dimensionality of Confinement.

Rib waveguides (2D confinement) offer a pragmatic balance for polymer/Si devices, while 3D structures like photonic crystals represent cutting-edge frontiers for ultra-compact quantum photonics.

1.6.2. Classification according to geometry [8]

Geometry	Structure	Confinement Mechanism	Advantages	Limitations
Rib	Raised strip on substrate	Index contrast (core > cladding)	• CMOS-compatible • Low bending loss	Polarization sensitivity
Strip (Ridge)	Freestanding ridge	Strong lateral index step (e.g., Si/air)	• High integration density • Small footprint	Scattering loss at sidewalls
Slot	Twin rails with nano-gap	Field enhancement in low-index slot	• 100× intensity in slot region	Sub-100 nm fabrication tolerance
Buried	Core embedded in cladding	Symmetric index profile	• Low propagation loss (<0.1 dB/cm)	Limited to compatible materials
3D Photonic Crystal	Periodic lattice (e.g., woodpile Si)	Photonic bandgap	• Lossless 90° bends • Slow light effects	Nanolithography challenges
Microresonators	Microdisks/rings (e.g., SiO_2 on Si)	Total internal reflection + whispering gallery modes	• Ultra-high Q-factors • Nonlinear efficiency	Temperature sensitivity

Table 1.2: Classification according to geometry.

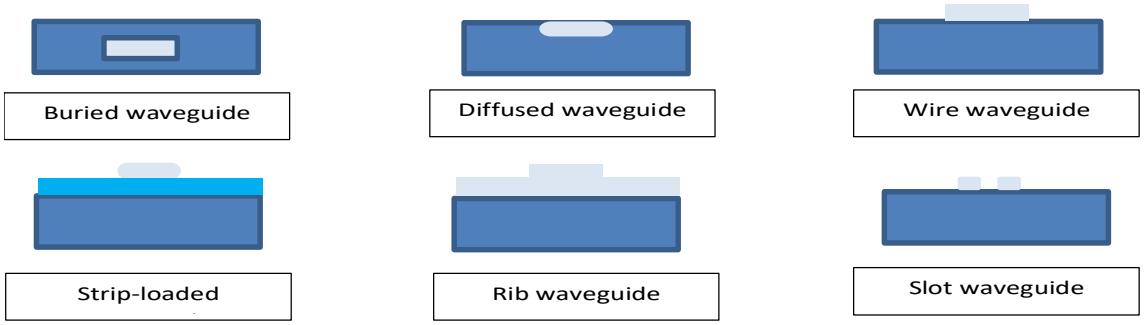

Figure 1.5: Schematic representation of various channel waveguides.

The previous figure shows a variety of famous 2D optical rectangular waveguides used any very large ranges of integrated photonics.

1.7. A brief overview on planar waveguides,2D waveguides and 3D waveguides:

1.7.1. Planar waveguides (1D Optical Confinement)

Planar waveguides form the foundational building blocks of integrated photonics, enabling light propagation confined in one spatial dimension while remaining unguided in the plane of the substrate. These structures, typically fabricated as thin dielectric films on semiconductor or glass substrates, are critical for applications ranging from on-chip optical interconnects to evanescent-field biosensors. Unlike fibers or channel waveguides, planar waveguides excel in scenarios requiring large-area light distribution or hybrid integration with electronic circuits. This chapter explores their modal characteristics, fabrication techniques, and loss mechanisms, with emphasis on design trade-offs between confinement strength, scattering losses, and coupling efficiency. Key material systems (e.g., silicon-on-insulator, doped silica, and polymers) are compared to highlight their suitability for visible, near-infrared, or mid-infrared operation.

1.7.2. 2D Waveguides (channel/rib Structures)

Two-dimensional waveguides, comprising channel (buried core), rib (ridge-on-slab), or loaded (high-index strip) geometries, enable optical confinement in both transverse dimensions (*x* and *y*) via refractive index contrast [5]. Single-mode operation is achieved when the waveguide width satisfies, while bending losses, inversely proportional to the bend radius, impose critical design constraints for photonic integrated circuits (PICs). Fabrication typically employs photolithography coupled with dry etching (RIE/DRIE) for high-precision silicon or silicon nitride structures, or wet etching, though direct writing via femtosecond lasers or e-beam lithography offers flexibility for complex geometries. Material selection governs operational bandwidth and loss: silicon ($n\approx3.5$) dominates telecom applications (1.55 μm), while low-loss Si_3N_4 ($n\approx2.0$) enables visible-to-NIR devices, and lithium niobate ($LiNbO_3$, $n\approx2.2$) facilitates electro-optic modulation (Bogaerts et al., 2020). Polymer waveguides (e.g., SU-8, $n\approx1.6$) provide mechanical flexibility for wearable photonics. These structures underpin advancements in silicon photonics (optical interconnects, modulators), quantum optics (entangled photon sources), and lab-on-a-chip systems (bio-sensing, spectroscopy).

1.7.3. 3D Waveguides (optical fibers & photonic crystal structures)

Three-dimensional waveguides achieve full spatial confinement through cylindrical symmetry (step-index fibers) or micro structured designs (photonic crystal fibers). Step-index fibers maintain a sharp refractive index contrast between core and cladding, while graded-index fibers reduce modal dispersion through parabolic index profiles. The normalized frequency determines single-mode operation ($V<2.405$), with attenuation in silica fibers reaching ultralow values (~0.2 dB/km at 1550 nm) through hydroxyl radical reduction. Photonic crystal fibers (PCFs), fabricated via stack-and-draw methods, utilize air-hole microstructures to enable novel dispersion engineering and bandgap guidance. Standard single-mode fibers (SMF) feature 8-10 μm cores, whereas multimode fibers (MMF) employ 50-100 μm cores for short-reach interconnects. These waveguides form the backbone of modern telecommunications

networks, while specialty variants enable high-power fiber lasers (>>kW) and minimally invasive endoscopic imaging through <250 μm diameter probes. Compared to planar/2D counterparts, 3D waveguides exhibit 6-orders-of-magnitude lower loss (0.0002 dB/km vs 0.1-1 dB/cm) but lack on-chip integration capabilities.

In the third chapter we would dive deeply in a selective 2D structure (an optical rib waveguide).

For the classification in order of the material nature; there are many ranges of materials each one has a certain way of fabrication and application.

1.8. Materials for optical waveguide fabrication [9]:

1.8.1. Core and cladding materials

- **Silica (SiO_2)**: Dominates telecom fibers due to ultra-low loss (~0.2 dB/km in near-IR). Germanium (GeO_2) dopants increase the core's refractive index, while fluorine (F) reduces the cladding's index.
- **Silicon (Si)**: High-index (n ≈ 3.5) core material for integrated photonics (e.g., silicon-on-insulator, SOI.
- **Polymers (SU-8, PMMA)**: Flexible, low-cost waveguides for biomedical/consumer optics; tunable refractive index (~1.4–1.6).
- **Lithium Niobate ($LiNbO_3$)**: Electro-optic tunability via the Pockels effect, used in modulators.
- **Chalcogenide Glasses (As_2S_3)**: Mid-IR transparency (up to 12 μm) for chemical sensing.

1.8.2. Substrates

- **Silicon (SOI)**: Standard substrate for CMOS-compatible photonics.
- **Glass (SiO_2)**: Used for planar lightwave circuits (PLCs).

1.9. Fabrication techniques and applications:

Waveguide structures are fabricated using various methods depending on the type (optical, microwave) and material (semiconductor, polymer, metal). Below is an organized overview of key fabrication techniques:

Since my work is all about optic waveguides, I will talk more about the fabrication techniques of optical waveguides

a. Photolithography and Etching: Depositing materials (e.g., Si, SiO_2, Si_3N_4) onto a substrate, patterning with photoresist using UV light and masks, and etching (dry/wet) to form waveguide channels. It has many applications such as Silicon photonics and integrated photonic circuits.it relies on these techniques: Reactive ion etching (RIE), deep RIE (DRIE).

b. Ion Exchange: Immersing glass in molten salts (e.g., Ag^+, K^+) to replace ions, creating refractive index changes. It has many applications such as Planar glass waveguides and fiber Bragg gratings.

c. Laser Direct Writing: Femtosecond lasers modify refractive indices in transparent materials (e.g., glass, crystals) . It has many applications such as 3D waveguides, photonic chips.

d. Thin-Film Deposition: Depositing layers via CVD, PVD, or sputtering, followed by patterning.By using **materials** like Silicon-on-insulator (SOI), lithium niobate ($LiNbO_3$).

e. Epitaxial Growth: Growing crystalline semiconductor layers (e.g., GaAs, InP) with varying compositions/doping. It has many applications such as Laser diodes and photonic integrated circuits.

f. Fiber Drawing: Heating and drawing a glass preform (core/cladding) into thin fibers.It has many applications such as Optical fiber communication.

g. Nanoimprint Lithography: Pressing a mold into polymer resist to imprint patterns. It has many applications such as Polymer waveguides, low-cost fabrication. [10]

These guides we are talking about are guiding light as it mentioned earlier so we need to have an overview about light and rays

1.10. Understanding light: rays, waves, and wave fronts [11] [12] [13]:

Light rays, governed by geometric optics (Snell's law), model light as straight-line paths ideal for large-scale systems like lenses and mirrors, but fail to explain wave phenomena (e.g., diffraction). Light waves, described by physical optics (Maxwell's equations), treat light as electromagnetic oscillations essential for small-scale interactions (e.g., wavelength-sized structures), enabling analysis of interference, polarization, and coherence. While rays simplify

designs for imaging systems, waves are indispensable for precision applications like fiber optics and nano-photonics. The choice between models hinges on whether the system's scale dwarfs the wavelength (rays) or matches it (waves).

Wave front and Rays For an electromagnetic wave, the wave front is represented as a surface of identical phase, and can be modified with conventional optics. A wave front is a surface passing through the points of a wave that have the same phase and amplitude. Ray is a line everywhere perpendicular (normal) to the surfaces of the constant phase of the wave - wave fronts. Rays point in a local direction of the propagation of the wave.

In optics it is sufficient to track just the rays, if one is interested in phenomena over distances larger than a wavelength of light. This is approximation of geometrical optics.

Planar wave has well-defined direction of propagation; thus, we can think about light rays Physicists say "we can use geometrical optics approximation here".

1.11. Guided modes [14]:

If $\theta < \theta_{c2} < \theta_{c3}$, the wave inside the core is totally reflected at both interfaces and is trapped by the core, resulting in guided modes. As the wave is reflected back and forth between the two interfaces, it interferes with itself. A guided mode can exist only when a transverse resonance condition is satisfied so that the repeatedly reflected wave has constructive interference with itself. In the core region, the x component of the wave vector is $k_1 \cos\theta$ for a ray with an angle of incidence θ, while the z component is $\beta = k_1 \sin\theta$.The phase shift in the optical field caused by a round-trip transverse passage in the core of thickness d is $2k_1 d \cos\theta$.In addition, there are phase shifts φ_2 and φ_3 associated with the internal reflections at the lower and upper interfaces, respectively.

There are two types of modes that could be present in a planar waveguide:

- Transverse electric (TE) modes have the electric field, but not the magnetic field perpendicular to the propagation direction. That means there is some longitudinal component of the magnetic field. They may also be called *H modes*.
- Transverse magnetic (TM) modes have the magnetic field, but not the electric field perpendicular to the propagation direction. That means there is some longitudinal component of the electric field. They may also be called *E modes*.

In the figure (1.6), we observe different modes of light propagation within a slab waveguide.

Mode (a), often representing the fundamental or lowest-order mode (M_0), is characterized by light rays propagating at a relatively steep angle (θ) with respect to the waveguide boundary. This results in minimal internal reflections and a field distribution with a single, broad peak confined predominantly within the high-refractive-index core (n_1). As the mode order increases, the angle of incidence (θ) decreases, leading to more frequent internal reflections and more complex field patterns.

Mode (b), illustrates a higher-order mode (M_1), where the light rays propagate at a shallower angle than in mode (a), leading to more reflections within the waveguide. This results in a field distribution that begins to show a "node" or zero-crossing within the core, indicating a more oscillatory pattern with two peaks.

Mode (c), depicts an even higher-order mode (M_2), characterized by a significantly shallower propagation angle and numerous internal reflections. This increased number of reflections corresponds to a field distribution with multiple nodes and peaks within the core, signifying a more complex and spread-out optical field compared to the lower-order modes. As the mode order increases (from a to c), the effective refractive index (n_{eff}) of the mode decreases, and the confinement of the light within the core generally becomes weaker, with more of the field extending into the surrounding cladding regions.

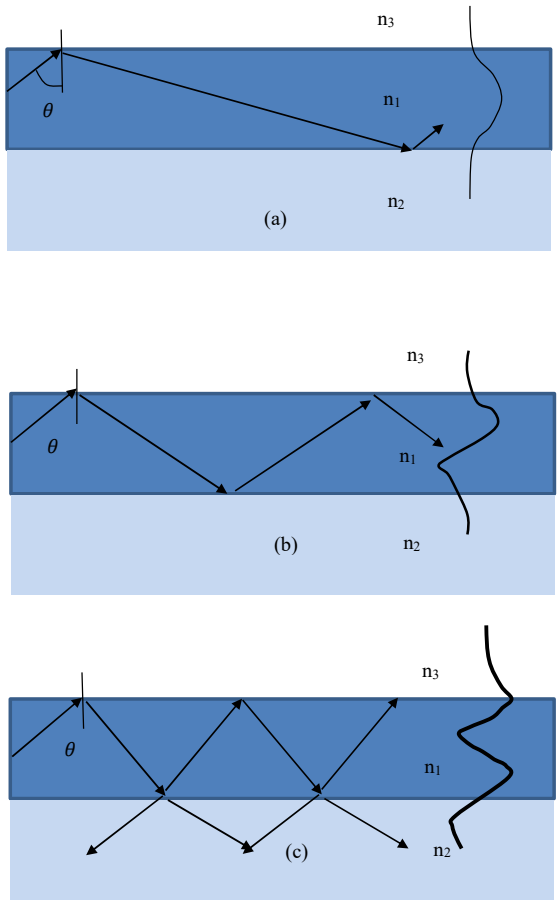

Figure1.6: Modes of an asymmetric planar step-index waveguide.

1.12. Definition of photonics [15]:

Photonics is the science and technology of generating, controlling, manipulating, and detecting photons (light particles) across the electromagnetic spectrum (UV to infrared). It encompasses the study of light's wave and quantum properties to develop devices and systems for applications such as telecommunications, sensing, computing, and energy. Photonics bridges classical optics with modern technologies like lasers, optical fibers, and integrated photonic circuits. It is the counterpart of electronics, replacing electrons with photons to harness light for practical applications.

It integrates optics with electronics to create systems where light is the primary information carrier.

1.13. Core principles of photonics [15]:

1.13.1. ***Light Propagation and Maxwell's Equations***

Light is an electromagnetic wave governed by Maxwell's equations. These describe how electric (**E**) and magnetic (**B**) fields propagate and interact with materials.

1.13.2. Waveguide Theory

Waveguides confine light via total internal reflection (TIR).

1.13.3. Light-Matter Interaction

Photons interact with materials via linear effects like refraction, absorption, and dispersion and a nonlinear effect such as Second-harmonic generation (SHG) and Kerr effect.

1.13.4. Quantum Nature of Light

The wave-particle duality of light, a fundamental tenet of quantum mechanics, posits that light simultaneously exhibits wave-like and particle-like properties. At the quantum scale, light manifests as discrete energy quanta called photons, with energy defined by $E=h\nu$, where h is Planck's constant and ν is the photon's frequency. This quantized nature underpins phenomena such as the photoelectric effect, where light-matter interaction occurs via photon absorption. Coherent states, exemplified by laser light, represent a quantum superposition of photon number states that approximate classical electromagnetic waves while retaining quantum mechanical attributes, such as phase stability and minimal amplitude noise. Beyond coherence, quantum entanglement a non-classical correlation between photons enables secure communication protocols like quantum key distribution (QKD), where entangled photon pairs ensure cryptographic security through the no-cloning theorem. These principles form the foundation of quantum photonics, driving advancements in single-photon detectors capable of resolving individual photons with high temporal precision and quantum efficiency. Such detectors are critical for quantum computing (e.g., photonic qubit readout), quantum communication networks, and precision metrology. By unifying wave and particle paradigms, these concepts redefine the technological limits of optical systems, bridging fundamental physics with transformative applications.

1.13. Methods and approximations for waveguide analysis:

Analytical and numerical methods are essential tools for designing waveguide-based devices, enabling the analysis and evaluation of wave propagation phenomena. Analytical solutions are not universally applicable to all waveguide structures, as they assume guiding structures are uniform along the propagation direction. Many waveguide configurations lack this uniformity, necessitating propagation-based numerical techniques. These methods accurately capture waveguiding properties and provide insight into field evolution. The choice of method depends on criteria such as structure geometry, initial conditions, accuracy requirements, and computational time.

1.13.1. Time-domain methods:

- ✓ Finite-Difference Time-Domain (FDTD).
- ✓ Split-Step Method (SSM).
- ✓ Finite Element Method (FEM).

1.13.2. Frequency-domain methods:

- ✓ Beam Propagation Method (BPM)
- ✓ Transfer Matrix Method (TMM)
- ✓ Eigenmode Expansion (EME)
- ✓ Plane Wave Expansion (PWE)

Here is a table that shows the type of each method mentioned before and its characteristics:

Method	Type	Domain	Characteristics
FDTD	Numerical	Time-domain	• Most general/rigorous for optical structures • Computationally intensive (especially 3D) • Ideal for 2D geometries
SSM	Numerical	Time-domain	• Solves nonlinear PDEs (e.g., nonlinear Schrödinger equation) • Separates linear (frequency/time domain) and nonlinear (time domain) steps • Used for nonlinear pulse propagation in fibers
FEM	Numerical	Frequency-domain	• Handles complex geometries/arbitrary cross-sections • Meshes domain into triangles/rectangles • Solves PDEs via variational or Galerkin approaches → Eigenvalue equations
BPM	Numerical	Frequency-domain	• Approximates scalar wave equation (small refractive index variations) • Subtypes: FFT-BPM, Finite-Difference BPM, Finite-Element BPM
PWE	Numerical	Frequency-domain	• Expands fields as frequency-defined states • Applicable to photonic crystals, resonators, dispersion relations
TMM	Numerical	Frequency-domain	• Simple formulation for multilayer planar waveguides • Computes transmission spectra and mode wave vectors via matrix eigenvalues • Handles complex refractive indices and graded-index structures

Table1.3: Comparative analysis of computational methods in photonics: types, domains and characteristics [16].

1.13.3.Effective Index Method (EIM)" Semi-analytical hybrid method" [17]

As this study focuses on the Effective Index Method (EIM), we provide a breakdown of the method below:

The EIM is a computational technique used primarily in waveguide optics and photonics to simplify the analysis of 2D and 3D structures (like optical fibers or planar waveguides) into a 1D problem. Here are its core analysis steps:

1. Divide the 2D or 3D waveguide cross-section into regions where one dimension can be treated as laterally uniform.

2. 1D Wave Equation Solution (Vertical) for each segmented region solve the 1D scalar wave equation vertically (in one direction) and extract the effective index for each region. This becomes the new "refractive index" for the lateral dimension.
3. Construct 1D Effective Index Profile (Lateral) by create a new 1D refractive index profile n_{EIM} using the effective indices n_{eff} obtained from each vertical region.
4. Solve 1D Wave Equation (Lateral); Solve the wave equation laterally using n_{EIM} and find the propagation constant β and lateral mode profile.
5. Combine solutions in order to find the whole structure effective index.

Chapter 2 provides a detailed theoretical explanation of EIM, including its mechanism for waveguide analysis.

1.14. Conclusion

This chapter has systematized waveguide photonics through three key pillars:

1. **Historical-material evolution**: From Maxwell's unification to nano-fabricated dielectric structures.
2. **Confinement taxonomy**: Classifying waveguides by dimensionality (planar/channel/volumetric), geometry (rib/slot/photonic crystal), and modal behavior (TE/TM).
3. **Computational trade-offs**: Contrasting time-domain (FDTD, SSM) and frequency-domain (FEM, BPM, PWE) methods for guided-wave modeling.

These foundations pivot toward Chapter two's focus: a rigorous theoretical exposition of the semi-analytical Effective Index Method (EIM) for 2D waveguide analysis, bridging historical principles with modern design methodologie.

Chapter 02: Planar Waveguide Analysis (Effective Index Method and Modes Characterizations).

2.1. Introduction

This chapter establishes the theoretical foundation for analyzing planar optical waveguides, essential components in integrated photonics and semiconductor lasers. We begin with Maxwell's equations the cornerstone of electromagnetic theory to derive wave propagation dynamics in dielectric media. The analysis focuses on slab waveguides (1D confinement) as a precursor to understanding rectangular rib waveguides (2D confinement) using the effective index method.

2.1. Maxwell equations:

Maxwell's equations, comprising the fundamental laws of electrodynamics, govern the behavior of electric (**E**) and magnetic (**H**) fields, as well as their interactions with matter through displacement (**D**) and induction (**B**) vectors.

$$\begin{cases} \vec{\nabla} \times \vec{E} + \dfrac{\partial \vec{B}}{\partial t} = \vec{0} \\ \vec{\nabla} \times \vec{H} - \dfrac{\partial \vec{D}}{\partial t} = \vec{J} \\ \vec{\nabla}.\vec{D} = \rho \\ \vec{\nabla}.\vec{B} = 0 \end{cases} \qquad (2.1)$$

These equations encompassing Gauss's laws for electricity and magnetism, Faraday's law of induction, and Ampère's law with Maxwell's addition uniquely determine electromagnetic fields even in charge- and current-free regions ($\rho = 0$, $\mathbf{J} = 0$), enabling the existence of self-sustaining electromagnetic waves. To resolve the fields in material media, constitutive relations ($\mathbf{D} = \varepsilon\mathbf{E}$, $\mathbf{B} = \mu\mathbf{H}$) are essential, where permittivity (ε) and permeability (μ) are tensorial in anisotropic materials but scalar in isotropic media. Strong fields, such as those from lasers, introduce nonlinear dependencies in ε and μ, critical for phenomena like optical harmonic generation. [14]

At boundaries between dissimilar media, continuity conditions emerge: the normal components of **B** and **D** (with **D**'s discontinuity equaling surface charge σ) and the tangential components of **E** and **H** (with **H**'s discontinuity equaling surface current **K**). In optical systems (e.g., dielectric waveguides, fibers), where σ and **K** vanish, **E**, **H**, **B**, and **D** exhibit full continuity, ensuring seamless wave propagation. These principles underpin modern photonic technologies, from fiber-optic communications to integrated photonic circuits, by rigorously defining how electromagnetic waves interact with material interfaces and propagate through structured media. [14]

2.3. Planar optical waveguides [14]:

Planar optical waveguides are the key devices to construct integrated optical circuits and semiconductor lasers. Generally, rectangular waveguides consist of a square or rectangular core surrounded by a cladding with lower refractive index than that of the core. Three-dimensional analysis is necessary to investigate the transmission characteristics of rectangular waveguides. However, rigorous three-dimensional analysis usually requires numerical calculations and does not always give a clear insight into the problem. Therefore, this chapter first describes two-dimensional slab waveguides to acquire a fundamental understanding of optical waveguides.

2.3.1. Slab waveguides

Dielectric slabs are the simplest optical waveguides.The figure below shows a typical example of a slab waveguide.It consists of a thin dielectric layer (the guiding layer or the core) sandwiched between two semi-infinite bounding media(clad).

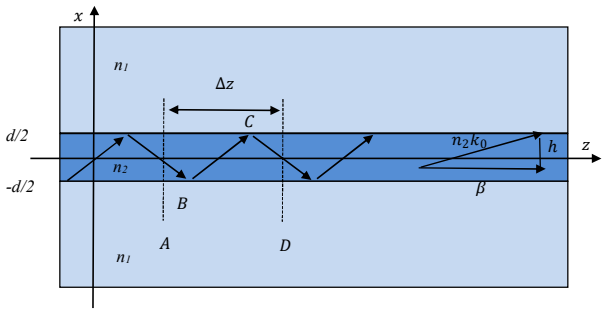

Figure2.1: Schematic drawing of a symmetric slab waveguide.

Generally,the index of refraction of the core must be greater than those of the surrounding media.

The following equation describes the index profile of a symmetric dielectric waveguide:

$$n_2 > n_1 \quad ; \quad n(x)\begin{cases} n_2, & |x| < \frac{d}{2} \\ n_1, & otherwise \end{cases} \quad (2.2)$$

With:

- d: Thickness of core.
- n_2: The index of refraction of the core.
- n_1: The index of refraction of the bounding media.

The problem at hand is to find these guided modes.

2.3.2. Unified theory of waveguides

All waveguides rely on solving Maxwell's equations under boundary conditions specific to their structure and frequency [24].

The electromagnetic treatment of such a problem is relatively easy because the medium is homogeneous in each segment of the dielectric structure.In addition, the solutions of Maxwell's equations in homogeneous media are simply plane waves.Thus all we need to do is write the plane wave solutions for each segment and then match the boundary conditions at the interfaces to ensure the continuity of the wavefunction.We now onsider the propagation of monochromatic radiation along the Z axis.Maxwell's equation can be written in the form:

$$\nabla \times \vec{H} = i\omega\varepsilon_0 n^2(x)\vec{E}$$

$$\nabla \times \vec{E} = i\omega\mu\vec{H} \qquad (2.3)$$

Solutions to the previous wave equations can be taken as:

$$E(x,t) = E_m(x)e^{i(\omega t-\beta z)}$$

$$H(x,t) = H_m(x)e^{i(\omega t-\beta z)} \ (2.4)$$

Where:

- β:is the z component of the wavevectors, known as the propagation constant to be determined from Maxwell's equations.
- $E_m(x)\ and\ H_m(x)$: are wavefunctions of the guided modes and m called the mode number (integer number).

For a layered dielectric structure that consists of homogeneous and isotropic materials,the wave equation can be obtained by eliminating H from equation (2.3):

$$\left(\frac{\partial^2}{\partial x^2}+\frac{\partial^2}{\partial y^2}\right)E(x,y) + [k_0^2 n^2(r) - \beta^2] \times E(x,y) = 0; k_0 = \frac{\omega}{c} \ (2.5)$$

k_0:The waveguide number in vacuum.

We will solve for this equation separately in each segment of the structure and then match the tangential components of the field vectors at each interface.

The propagation constant β is a very important parameter because it determines whether the field varies sinusoidally or exponentially.

For confined modes, the field amplitude must fall off exponentially outside the guide structure.

The propagation constant β of a confined mode must be such that:

$\frac{n_1\omega}{c} < \beta < \frac{n_2\omega}{c}$.(2.6).

Thus confined modes whose propagation constant satisfies these conditions (equation (2.6)) will be found.

The modes can be classified as either either TE or TM modes.

- The TE modes have the field components $E_y, H_x$and H_z.
- The TM modes have the field components $H_y, E_x$and E_z.

2.3.3. Guided TE modes

the electric field amplitude of the guided TE modes can be written in the form:

$$E_y(x,z,t) = E_m(x)e^{[i(\omega t - \quad)]} \tag{2.7}$$

The mode function $E_m(x)$ is taken as:

$$E_m(x) = \begin{cases} A\sin(hx) + B\cos(hx), & |x| < \frac{1}{2}d \\ Ce^{(-qx)}, & x > \frac{1}{2}d \\ De^{(qx)}, & x < -\frac{1}{2}d \end{cases} \tag{2.8}$$

- A,B,C and D are constants.

The parameters h and q are related to the propagation constant by:

$$h = [\left(\frac{n_2\omega}{c}\right)^2 - \beta^2]^{\frac{1}{2}}$$

$$q = [\beta^2 - \left(\frac{n_1\omega}{c}\right)^2]^{\frac{1}{2}} \tag{2.9}$$

The parameter h may be considered as the transverse component of the wavevector in the guiding layer.

To have acceptable solutions,$E_y$and $H_z$must be continuous at the interfaces.

Since $H_z = (\frac{i}{\omega\mu})(\frac{\partial E_y}{\partial x})$,it is a must to match the magnitude as well as the slope of the TE mode functions $E_m(x)$ at the interfaces.

This leads to:

$$A\sin\left(\frac{1}{2}hd\right) + B\cos\left(\frac{1}{2}hd\right) = Ce^{\left(-\frac{1}{2}qd\right)} \tag{2.10}$$

$$hA\cos\left(\frac{1}{2}hd\right) - hB\sin\left(\frac{1}{2}hd\right) = -qCe^{(-\frac{1}{2}qd)} \tag{2.11}$$

$$-A\sin\left(\frac{1}{2}hd\right)+B\cos\left(\frac{1}{2}hd\right)=De^{\left(-\frac{1}{2}qd\right)} \qquad (2.12)$$

$$hA\cos\left(\frac{1}{2}hd\right)+hB\sin\left(\frac{1}{2}hd\right)=qDe^{\left(-\frac{1}{2}qd\right)} \qquad (2.13)$$

from which we obtain:

$$2A\sin\left(\frac{1}{2}hd\right)=(C-D)e^{\left(-\frac{1}{2}qd\right)} \qquad (2.14)$$

$$2hA\cos\left(\frac{1}{2}hd\right)=-q(C-D)e^{\left(-\frac{1}{2}qd\right)} \qquad (2.15)$$

$$2B\cos\left(\frac{1}{2}hd\right)=(C+D)e^{\left(-\frac{1}{2}qd\right)} \qquad (2.16)$$

$$2hB\sin\left(\frac{1}{2}hd\right)=q(C+D)e^{\left(-\frac{1}{2}qd\right)} \qquad (2.17)$$

There are two sets of solutions found:

a. Symmetric modes (A=0 and C=D)

$$h\tan\left(\frac{1}{2}hd\right)=q \quad \text{(for symmetric TE modes)} \qquad (2.18)$$

b. Antisymmetric modes (B=0 and C=-D)

$$h\cot\left(\frac{1}{2}hd\right)=-q \quad \text{(for antisymmetric TE modes)} \qquad (2.19)$$

These two last equations can be combined into a single equation:

$$\tan(hd)=\frac{2hq}{h^2-q^2} \qquad (2.20)$$

The solutions of TE modes are divided into two classes,the first class:

$$A=0, C=D,\ h\tan\left(\frac{1}{2}hd\right)=q \qquad (2.21)$$

The second class:

$$B=0, C=-D,\ h\cot\left(\frac{1}{2}hd\right)=-q \qquad (2.22)$$

The propagation constants of the TE modes are found from a numerical or graphical solution of Equations (2.21) and (2.22), with the definition of h and q given by Equation (2.9). A very simple and well-known graphic solution is described here, since it clearly shows the way in which the number of TE modes depends on both the thickness d and the difference of indices of refraction. By putting $u=\frac{1}{2}hd$ and $v=\frac{1}{2}qd$, Equation (2.21) becomes $u\tan u=v$, with:

$$u^2+v^2=(n_2^2-n_1^2)\left(\frac{\omega d}{2c}\right)^2=(n_2^2-n_1^2)(\frac{\pi d}{\lambda})^2 \qquad (2.23)$$

The propagation constants of confined TE modes in a symmetric slab waveguide are determined by the intersections of curves $v=u\tan u$ (for even modes) or $v=-u\cot u$ (for odd modes) with a circular contour of radius $V=\sqrt{n_2^2-n_1^2}(\pi d/\lambda)$ in the uv-plane. The number of

supported modes depends on V: smaller V (e.g., V=1.2) yields fewer modes (e.g., TE_0), while larger V (e.g., V=5) allows more modes (e.g., four TE modes). For V between 0 and $\pi/2$, only the first-class (even) mode exists; higher V introduces alternating classes (even and odd).

Wavefunctions exhibit symmetry due to the symmetric refractive index profile $n(x)$: even modes (zero slope at x=0) resemble $\cos(hx)$, and odd modes (zero value at x=0) resemble $\sin(hx)$, both decaying exponentially outside the core ($|x|>d/2$). The m-th mode has $m-1$ nodes. For example, a waveguide with n_2=1.6, n_1=1.5, d=5μm, and λ=1.55μm yields V=5.64, supporting four TE modes. Solutions are obtained by matching wavefunction values and slopes at the core-cladding boundary ($|x|=d/2$).

A symmetrical slab waveguide with parameters n_2=1.6, n_1=1.5, core thickness d=5μm, and wavelength λ=1.55μm supports four TE modes. The normalized propagation constants ($\hat{\beta}$) for these modes are 1.5946, 1.5785, 1.5521, and 1.5175, with the fundamental mode (lowest-order) having the largest value, indicating the highest phase velocity. Confinement factors (Γ), representing the fraction of energy inside the core, decrease from 0.9914 (fundamental mode) to 0.7511 for higher-order modes.

The normalized propagation constant $\hat{\beta}=\beta/(\omega/c)$ is equivalent to the effective refractive index n_{eff}, defined as $n_{eff}=c/v_p$, where $v_p=\omega/\beta$ is the phase velocity. For confined modes, n_{eff} lies between n_1 and n_2, ensuring guided propagation. This parameter simplifies mode comparison and highlights the phase velocity's dependence on the waveguide's refractive indices.

2.3.4. Guided TM modes

we consider the TM modes whose magnetic field vector is perpendicular to the plane of propagation (xz plane). The derivation of the confined TM modes is similar in principle to that of the TE modes.

The field amplitudes are written:

$$H_y(x,z,t) = H_m(x)e^{[i(\omega t-\beta z)]} \qquad (2.24)$$

$$E_x(x,z,t) = \left(\frac{i}{\omega\mu}\right)\left(\frac{\partial H_z}{\partial z}\right) \qquad (2.25)$$

$$E_z(x,z,t) = \left(-\frac{i}{\omega\mu}\right)\left(\frac{\partial H_y}{\partial x}\right) \qquad (2.26)$$

The wavefunction $H_m(x)$ is:

$$H_m(x)\begin{cases} A\sin hx + B\cos hx\,, |x| < \frac{1}{2}d \\ Ce^{(-qx)} \quad , x > \frac{1}{2}d \\ De^{(qx)} \quad , x < -\frac{1}{2}d \end{cases} \qquad (2.27)$$

And:

$$h\tan\left(\frac{1}{2}hd\right) = \frac{n_2^2}{n_1^2}q \text{(for even solutions)} \qquad (2.28)$$

$$h\cot\left(\frac{1}{2}hd\right) = -\frac{n_2^2}{n_1^2}q \text{(for odd solutions)} \qquad (2.29)$$

those lead to:

$$\tan(hd) = \frac{2h\bar{q}}{h^2-\bar{q}^2}; \bar{q} = \frac{n_2^2}{n_1^2}q \qquad (2.30)$$

Equations (2.28) and (2.29), governing mode propagation, can be solved graphically by analyzing intersections of curves (e.g., $v=u\tan u$) with a circular contour of radius V.

- **Fundamental Modes**: TE00 and TM00 modes have no cutoff frequency and remain confined for all V.
- **Higher-Order Modes**: TE11 and TM11 modes cut on at V=π/2.
- **Low Frequency ($V<\pi/2$)**: Only TE00 and TM00 modes are supported.
- **Moderate Frequency ($\pi/2<V<\pi$)**: TE11 and TM11 modes become supported in addition to the fundamental modes.

2.4. TE and TM confined modes in asymmetric slab waveguide [14]:

In practice most slab waveguides are not symmetric. In this section, we treat the confined modes in asymmetric slab waveguides. The symmetric slab waveguides described in the last section may be viewed as a special case of the asymmetric ones.

Considering the propagation of confined modes in an asymmetric slab waveguide whose index profile is given by:

$$n(x) = \begin{cases} n_1 & 0 < x \\ n_2 & -t < x < 0 \\ n_3 & x < -t \end{cases} \quad (2.31) \quad \text{with: } n_3 < n_2 < n_3$$

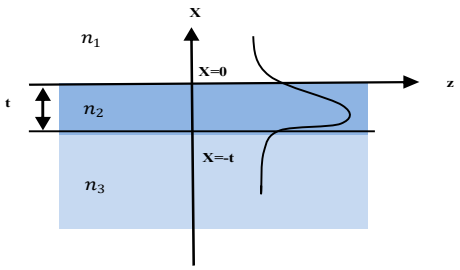

Figure2.2: Schematic drawing of an asymmetric slab waveguide with a core index of n_2.

- t=The thickness of the guiding layer.

To be a satisfactory wavefunction, a solution to Maxwell's wave equation must be continuous, single valued and finite through the space.

We will first examine the physical nature of the solution as a function of the propagation constant β at a fixed frequency ω.

For $\beta > n_2(\frac{\omega}{c})$ we have $(\frac{1}{E})(\frac{\partial^2 E}{\partial x^2})$.

Confined guided modes exist when $n_3(\omega/c) < \beta < n_2(\omega/c)$, requiring the core (layer 2) to have the highest refractive index.

- ✓ Fields decay exponentially outside the core, analogous to quantized states in a potential well.
- ✓ Energy is confined near the guiding layer (minimal leakage).
- ✓ Discrete β values; number of modes increases with core thickness t, frequency, and refractive indices.

Substrate radiation modes occur when $n_1(\omega/c) < \beta < n_3(\omega/c)$.

- ✓ Exponential decay in substrate ($x>0$), sinusoidal elsewhere.
- ✓ Most energy flows in the substrate.

Radiation modes exist for $\beta < n_1(\omega/c)$ it is sinusoidal in all regions so the energy radiates freely.

2.4.1. Guided TE modes

For TE modes, the electric field vector is perpendicular to the plane of incidence (xz plane).Thus Ey is the only component of the electric field vector. The field component Ey of the TE mode can be taken in the form

$$E_y(x, y, z, t) = E_m(x)e^{[i(\omega t - \beta z)]} \quad (2.32)$$

where β is the propagation constant and $Em(x)$ is the wavefunction of the mth mode.

The function $Em(x)$ assumes the following forms in each of the three regions:

$$E_m(x)\begin{cases} Ce^{(-qx)} & , \ 0 \le x \\ C\left[\cos hx - \frac{q}{h}\sin hx\right] & , -t \ \le x \le 0 \\ C\left[\cos ht + \frac{q}{h}\sin ht\right] e^{[p(x+t)]} & , x \le -1 \end{cases} \quad (2.33)$$

- C=normalization constant.
- And h, q and p are given by:

$$h = [\left(\frac{n_2\omega}{c}\right)^2 - \beta^2]^{\frac{1}{2}} \ , q = [\beta^2 - \left(\frac{n_1\omega}{c}\right)^2]^{\frac{1}{2}} \ , p = [\beta^2 - \left(\frac{n_3\omega}{c}\right)^2]^{\frac{1}{2}} \quad (2.34)$$

E_y and $H_z = \left(\frac{i}{\omega\mu}\right)(\frac{\partial E_y}{\partial x})$ must be continuous at x=0 and x=−t.

The wavefunction in Equation (2.33) ensures E_y is continuous at both interfaces, and $\frac{\partial E_y}{\partial x}$ is continuous at x=0.

Imposing continuity of $\frac{\partial E_y}{\partial x}$ at x=−t leads to:

$$h\sin(ht) - q\cos(ht) = p(\cos(ht) + \frac{q}{h}\sin(ht)) \quad (2.35)$$

Simplifying, the mode condition becomes:

$$\tan(ht) = \frac{p+q}{h(1-\frac{pq}{h^2})} \quad (2.36)$$

The propagation constant β for guided TE modes must satisfy this equation.

For a slab waveguide with refractive indices n_1, n_2,n_3, Equation (2.36) yields a finite number of solutions for β if the core thickness t is sufficiently large.

These modes are mutually orthogonal.

The constant C in $E_m(x)$ is chosen so that the field corresponds to 1 W of power flow per unit width (y-direction) along the z-axis.

A mode with E_y=$AE_m(x)$ carries a power flow of $|A|^2 W/m$.

The normalization condition is defined as:

$$S_z = \frac{1}{2}\int Re[E \times H^*]_z dx = 1 \quad (2.37)$$

Or equivalently,

$$-\frac{1}{2}\int_{-\infty}^{+\infty} E_y H_x^* dx = \frac{\beta_m}{2\omega\mu}\int_{-\infty}^{+\infty}[E_m(x)]^2 dx = 1 \qquad (2.38)$$

where *m* denotes the *m* th confined TE mode (corresponding to the *m* th eigenvalue of Equation (2.36) and $H_x = -i(\omega\mu)^{-1}\frac{\partial E_y}{\partial z}$. Substitution of Equation (2.33) for the wavefunction in Equation (2.38) and carrying out the integration lead to, after a few steps of algebraic manipulation,

$$C_m = 2h_m\left(\frac{\omega\mu}{|\beta_m|\left[t+\left(\frac{1}{q_m}\right)+\left(\frac{1}{p_m}\right)\right]\times(h_m^2+q_m^2)}\right)^{\frac{1}{2}} \qquad (2.39)$$

The orthonormalization of the modes can be written

$$\int_{-\infty}^{+\infty} E_m E_l dx = \frac{2\omega\mu}{|\beta_m|}\delta_{l,m} \qquad (2.40)$$

Where $\delta_{l,m}$ is a Kronecker delta.

2.4.2. Guided TM modes

For TM modes, the magnetic field vector is perpendicular to the plane of incidence (*xz* plane).

The derivation of the confined TM modes is similar in principle to that of the TE modes. The field components are:

$$H_y(x,z,t) = H_m(x)e^{[i(\omega t-\beta z)]} \qquad (2.41)$$

$$E_x(x,z,t) = \left(\frac{i}{\omega\mu}\right)\left(\frac{\partial H_z}{\partial z}\right) = \frac{\beta}{\omega\mu}H_m(x)e^{[i(\omega t-\beta\ )]} \qquad (2.42)$$

$$E_z(x,z,t) = \left(-\frac{i}{\omega\mu}\right)\left(\frac{\partial H_y}{\partial x}\right) \qquad (2.43)$$

The function *Hm*(*x*) assumes the following forms in each of the three regions:

$$H_m(x)\begin{cases} -C\left(\frac{h}{\bar{q}}\cos(ht)+\sin(ht)\right)e^{p(x+t)} & ,\ x \le -t \\ C\left(-\frac{h}{q}\cos(hx)+\sin(hx)\right) & ,-t \le x \le 0 \\ -\frac{h}{\bar{q}}Ce^{-qx} & ,\ 0 \le x \end{cases} \qquad (2.44)$$

where *C* is a normalization constant, *h*, *q*, and *p* are given by Equation (2.34), and $\bar{q}$ is defined as follows.

The continuity of *Hy* and *Ez* at the two interfaces leads, in a manner similar to Equation (2.36), to the eigenvalue equation

$$\tan(ht) = \frac{h(\bar{p}+\bar{q})}{(h^2-\bar{p}\bar{q})} \qquad (2.45)$$

Where $\bar{p} = \frac{n_2^2}{n_3^2}p$ and $\bar{q} = \frac{n_2^2}{n_1^2}q$.

We have $$\frac{1}{2}\int_{-\infty}^{+\infty} H_y E_x^* \, dx = \frac{\beta_m}{2\omega}\int_{-\infty}^{+\infty} \frac{H_m^2(x)}{\varepsilon(x)} dx = 1 \qquad (2.46)$$

Or using $n^2(x) = \frac{\varepsilon(x)}{\varepsilon_0}$:

$$\int_{-\infty}^{+\infty} \frac{|H_m(x)|^2}{n^2(x)} dx = \frac{2\omega\varepsilon_0}{\beta_m} \qquad (2.47)$$

Carrying out the integration using equation (2.44) gives

$$C_m = 2\sqrt{\frac{\omega\varepsilon_0}{|\beta_m| t_{eff}}} \qquad (2.48)$$

And $$t_{eff} = \frac{\bar{q}^2+h^2}{\bar{q}^2}\left(\frac{t}{n_2^2} + \frac{q^2+h^2}{\bar{q}^2+h^2}\times\frac{1}{n_1^2 q} + \frac{p^2+h^2}{\bar{p}^2+h^2}\times\frac{1}{n_3^2 p}\right)$$

Generally, a mode becomes confined above a certain (cutoff) value of t/λ. At the cutoff value, $p=0$ and $\beta=n_3\omega/c$, and the mode extends to $x=-\infty$. According to the mode conditions (2.36), (2.45), and (2.34), cutoff values of t/λ for TE and TM modes are given, respectively, by

$$\left(\frac{t}{\lambda}\right)_{TE} = \frac{1}{2\pi\sqrt{n_2^2-n_3^2}} \times \left[m\pi + \tan^{-1}\left(\frac{n_3^2-n_1^2}{n_2^2-n_3^2}\right)^{1/2}\right] \qquad (2.49)$$

$$\left(\frac{t}{\lambda}\right)_{TM} = \frac{1}{2\pi\sqrt{n_2^2-n_3^2}} \times \left[m\pi + \tan^{-1}\frac{n_2^2}{n_1^2}\times\left(\frac{n_3^2-n_1^2}{n_2^2-n_3^2}\right)^{1/2}\right] \qquad (2.50)$$

where m is an integer (m=0,1,2,3,…) that denotes the m th confined TE (or TM) mode. Note that the cutoff thickness of the TM_m mode is always larger than that of the TE_m mode because $n_1<n_2$. For values of t/λ slightly above the cutoff value, $p\geq 0$, and the mode is poorly confined. As the values of t/λ increase, so does the value of p, and the mode becomes increasingly confined to layer 2. This is reflected in the normalized propagation constant or the effective index, $\beta\lambda/2\pi$, which at cutoff is equal to n_3 and for large t/λ approaches n_2. In a symmetric waveguide ($n_1=n_3$), the lowest order modes TE_{00} and TM_{00} have n_o cutoff and are confined for all values of t/λ. The confinement is, however, poor when t/λ becomes small.

The total number of confined modes that can be supported by a waveguide depends on the value of t/λ. To study the number of confined modes, we defined the parameter

$$V = \frac{\pi t}{\lambda}\sqrt{n_2^2 - n_3^2} \qquad (2.51)$$

Let's consider what happens about the TE modes in a given waveguide (i.e., fixed n_1, n_2, n_3, and t) as the wavelength of the light decreases gradually, assuming that the medium remains transparent and the indices of refraction n_1, n_2, and n_3 do not vary significantly. Since $\omega/c=2\pi/\lambda$, the effect of decreasing the wavelength is to increase the value of ω/c. At long wavelengths (low frequencies), such that

$$0 < V < \frac{1}{2}\tan^{-1}\left(\frac{n_3^2-n_1^2}{n_2^2-n_3^2}\right)^{1/2} \qquad (2.52)$$

the value of t/λ is below the cutoff value, and no confined mode exists in the waveguide. As the wavelength decreases such that

$$\frac{1}{2}\tan^{-1}\left(\frac{n_3^2-n_1^2}{n_2^2-n_3^2}\right) < V < \frac{\pi}{2} + \frac{1}{2}\tan^{-1}\left(\frac{n_3^2-n_1^2}{n_2^2-n_3^2}\right)^{1/2} \qquad (2.53)$$

one solution exists to the mode condition (2.36). The mode is designated as TE_{00} and has a transverse h parameter falling within the range:$0<ht<\pi$

so that it has no zero crossings in the interior of the guiding layer ($-t<x<0$). When the wavelength decreases further such that the parameter falls within the range

$$\frac{\pi}{2} + \frac{1}{2}\tan^{-1}\left(\frac{n_3^2-n_1^2}{n_2^2-n_3^2}\right)^{\frac{1}{2}} < V < \pi + \frac{1}{2}\tan^{-1}\left(\frac{n_3^2-n_1^2}{n_2^2-n_3^2}\right)^{\frac{1}{2}} \qquad (2.54)$$

the mode condition (2.36) yields two solutions. One corresponds to a value of $ht<\pi$ and is thus that of the lowest order TE_{00} mode. In the second mode,

$$\pi<ht<2\pi \qquad (2.55)$$

and, consequently, it has one zero crossing (i.e., the point where $Ey=0$) in the guiding region ($-t<x<0$). This is the so-called TE_{11} mode. Both of these modes correspond to the same frequency and can thus be excited simultaneously by the same input field. We notice, however, that the TE_{00} mode has a larger value of p (i.e., $p_0>p_1$) and is therefore more tightly confined to the guiding slab. It follows from Equation (2.34) that $\beta_0>\beta_1$, so that the phase velocity $v_0=\omega/\beta_0$ of the TE_{00} mode is smaller than that of the TE_{11} mode. We can now generalize and state that the m th mode (TE or TM) satisfies

$$(m-1)\pi<ht<m\pi \qquad (2.56)$$

and has $m-1$ zero crossings in the guiding layer ($-t<x<0$). The general features of TM modes are similar to those of TE modes, except that the corresponding values of p are somewhat smaller, indicating a lesser degree of confinement. A larger fraction of the total

TM mode power thus propagates in the outer medium compared to a TE mode of the same order.

2.4.3. Mode Confinement Factor

The electric field and magnetic field of confined modes are finite in the cladding regions. Although the power associated with the mode is propagating along the *z* direction, part of the electromagnetic field energy is actually propagating outside the guiding layer. Let Γ_i be the fraction of power flowing in medium *i* (*i*=1,2,3) of the slab waveguide. By definition, we have

$$\Gamma_i=\frac{Re\int_i(E\times H^*)zdx}{Re\int_{-\infty}^{+\infty}(E\times H^*)zdx},\ (i=1,2,3) \qquad (2.57)$$

where the integral in the numerator is carried out over the *I* th layer.Γ_2 is the fraction of mode power flowing in the guiding layer n_2 and is often called the mode confinement factor. The mode functions derived earlier in this section can be employed for calculation of the confinement factor.

For TE modes Γ values are defined as:

$$\Gamma_1=\frac{\frac{1}{q}}{t+\frac{1}{q}+\frac{1}{p}}\times\frac{h^2}{h^2+q^2} \qquad (2.58)$$

$$\Gamma_2=\frac{t}{t+\frac{1}{q}+\frac{1}{p}}+\frac{\frac{1}{p}}{t+\frac{1}{p}+\frac{1}{q}}\times\frac{p^2}{h^2+q^2}+\frac{\frac{1}{q}}{t+\frac{1}{q}+\frac{1}{p}}\times\frac{q^2}{h^2+q^2} \qquad (2.59)$$

$$\Gamma_3=\frac{\frac{1}{p}}{t+\frac{1}{q}+\frac{1}{p}}\times\frac{h^2}{h^2+q^2} \qquad (2.60)$$

And $\Gamma_1+\Gamma_2+\Gamma_3=1$.

For TM modes Γ values are defined as:

$$\Gamma_1=\frac{\frac{1}{q'}}{t+\frac{1}{q'}+\frac{1}{p'}}\times\frac{h^2}{h^2+q^2} \qquad (2.61)$$

$$\Gamma_2=\frac{t'}{t'+\frac{1}{q'}+\frac{1}{p'}}+\frac{\frac{1}{p'}}{t'+\frac{1}{p'}+\frac{1}{q'}}\times\frac{p^2}{h^2+q^2}+\frac{\frac{1}{q'}}{t'+\frac{1}{q'}+\frac{1}{p'}}\times\frac{q^2}{h^2+q^2} \qquad (2.62)$$

$$\Gamma_3=\frac{\frac{1}{p'}}{t'+\frac{1}{q'}+\frac{1}{p'}}\times\frac{h^2}{h^2+q^2} \qquad (2.63)$$

Where:

$t'=\frac{t}{n_2^2};\frac{1}{q'}=\frac{q^2+h^2}{\bar{q}^2+h^2}\times\frac{1}{n_1^2q}$ and $\frac{1}{p'}=\frac{p^2+h^2}{\bar{p}^2+h^2}\times\frac{1}{n_3^2p}$

2.5. Effective index theory [14]:

Although simple layered structures such as dielectric slabs can be used for waveguiding purposes, the confinement of energy is only limited to one dimension. In practice, more complicated waveguide structures are used. For example, the waveguides used in integrated optics or guided-wave optics (also known as planar light circuits (PLCs)) are usually two-dimensional waveguides (e.g., channel waveguides, ridge waveguides). Figure (2.3) shows examples of such two-dimensional waveguides. Exact analytical treatment of these waveguide structures is not possible, except for some special cases. Although numerical solutions can be obtained by various methods, there are several approximate analytical approaches. Here, we will introduce one of the simplest approaches, the effective index theory.

Referring to Figure (2.3c), we consider the guiding of electromagnetic radiation in a ridge waveguide. The rectangular waveguide shown in Figure (2.3b) can be considered as a special case of this ridge waveguide by taking d=0, where d is the thickness of the guiding layer on both sides of the ridge. The thickness of the guiding layer at the ridge is t, which is chosen to be greater than d because we are interested in the confinement of electromagnetic radiation at the ridge. The width of the ridge is a. For confined propagation, the index of refraction n_2 is greater than either n_1 or n_3.

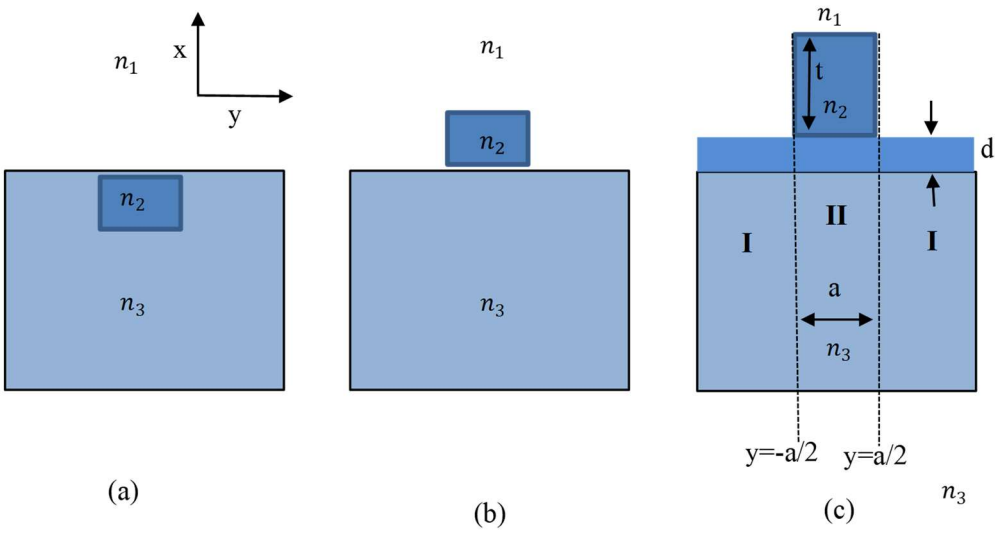

Figure2.3: Schematic drawing of several two-dimensional waveguides: (a) a rectangular strip of dielectric medium embedded in another dielectric medium of lower index of refraction; (b) ridge waveguide structure; and (c) another ridge structure.

We now divide the structure (2.3c) into three regions for the purpose of introducing the concept of effective index theory.

These regions are $y < -\frac{1}{2}a, -\frac{1}{2}a < y < \frac{1}{2}a$, and $\frac{1}{2}a < y$. In each of the three regions, the confinement along the vertical direction (x) is exactly identical to that of the asymmetric slab waveguide. For simplicity, we assume that only one TE mode is supported by all three regions of the dielectric structure. The propagation constant of the confined mode inside the ridge is, however, different from those on both sides of the ridge because of the difference in layer thickness. The effective index of refraction (or the normalized propagation constant) for these three segments is:

$$n_{eff}(y) = \begin{cases} n_I & y < -\frac{1}{2}q \\ n_{II} & -\frac{1}{2}a < y < \frac{1}{2}a \\ n_I & \frac{1}{2}a < y \end{cases} \qquad (2.64)$$

where n_I and n_{II} are the effective indices of refraction of the asymmetric slab waveguides, respectively.

In the theory of effective index, the lateral waveguiding is treated by taking Equation (2.64) as a "slab" waveguide structure along the y direction. Thus confinement of

electromagnetic radiation requires that $n_{II} > n_I$. This is always true when the thickness t is greater than d because, the effective index of refraction of any confined mode is an increasing function of thickness.

The main goal of this method is to Decompose the 2D/3D waveguide problem into 1D slab waveguide problems.

Starting from Maxwell's wave equation:

$$\nabla^2\psi + k_0^2 n^2 \psi = 0 \qquad (2.65) \qquad ,\psi = \psi(x,y)$$

Assuming that F(x) and G(y) are independent $\psi(x,y) = F(x)G(y)$

$$\left[\frac{\partial^2}{\partial x^2} + \frac{\partial^2}{\partial y^2} + \frac{\partial^2}{\partial z^2}\right] F(x)G(y) + (k_0 n)^2 \times F(x)G(y) = 0 \quad (2.66)$$

Where $\frac{\partial}{\partial z} = -j\beta$

As a result

$$G\frac{\partial^2 F}{\partial x^2} + F\frac{\partial^2 G}{\partial y^2} - \beta^2 FG + (k_0 n)^2 FG = 0 \qquad (2.67)$$

Dividing (2.67) by $\psi(x,y)\ or\ by\ F(x)G(y)$

$$\frac{1}{F}\frac{\partial^2 F}{\partial x^2} + \frac{1}{G}\frac{\partial^2 G}{\partial y^2} - \beta^2 + (k_0 n)^2 = 0 \qquad (2.68)$$

Where $\beta^2 + (k_0 n)^2 = cte.$

$$\frac{1}{F}\frac{\partial^2 F}{\partial x^2} + (k_0 n)^2 = \left(k_0 n_{eff}\right)^2 \qquad (2.69)$$

$$\frac{1}{G}\frac{\partial^2 G}{\partial y^2} - \beta^2 = -\left(k_0 n_{eff}\right)^2 \qquad (2.70)$$

n_{eff} is not the effective index of the whole structure.

$$\frac{\partial^2 F}{\partial x^2} + [(k_0 n)^2 - \beta^2]F = 0 \qquad (2.71)$$

$$\frac{\partial^2 F}{\partial x^2} + \gamma^2 F = 0 \qquad (2.72)$$

(2.72) represents the slab waveguide equation.

The solutions would be F(x) and n_{eff}.

After the rotation of the slab we have, we move on into the next direction (y).

$$\frac{\partial^2 G}{\partial y^2} + [\left(k_0 n_{eff}\right)^2 - \beta^2]G = 0 \qquad (2.73)$$

In order to find solutions, we need to go through both TE and TM modes in the directions x and y on a row so we can obtain:

$$\psi(x, y) = E_{y1}(x) \times E_{y2}(y) \qquad (2.74)$$

Where we can identify the modes present in the waveguide numerically. In this study we will use Maple as a software tool to analyze optic waveguides.

2.6. Conclusion

This chapter has systematically developed the theoretical tools for planar waveguide analysis:

1. Maxwell's equations govern light propagation, with boundary conditions defining mode continuity at interfaces.
2. Slab waveguides (symmetric/asymmetric) support discrete TE/TM modes, where the effective index n_{eff} scales with core thickness and index contrast. Cutoff conditions (V-parameter) dictate single/multi-mode operation.
3. Effective Index Method simplifies 2D waveguide analysis by decoupling vertical/lateral confinement, validated via mode orthogonality and normalization.

These principles enable efficient modeling of photonic devices from ridge waveguides to electro-optic modulators balancing accuracy with computational practicality. In subsequent chapters, we apply EIM to optimize rib waveguides, leveraging confinement physics for enhanced performance in integrated circuits.

Chapter 03: Results and Discussions.

3.1. Introduction

Rib waveguides stand as pivotal components in integrated photonics, enabling efficient light confinement for applications spanning telecommunications, sensing, and quantum computing. This chapter advances the theoretical framework established in Chapter 2 by applying the effective index method (EIM) to rigorously analyze rib waveguide performance. We begin by contextualizing critical terms dispersion**,** refractive index contrast, and mode classification that underpin our results discussion.

In order to mention and discuss results,we need to be aware of some terms such as dispersion,contrast and classification of waveguide by mode structure.

3.2. Rib waveguide [18] [19]:

3.2.1. Structure of rib Waveguides

A rib waveguide is a type of dielectric optical waveguide characterized by a raised strip (the "rib") on a planar substrate. It consists of three layers:

- Core: The rib (higher refractive index material, e.g., Si, polymer, or GaAs).
- Cladding: Surrounding material (lower refractive index, e.g., SiO_2, air, or organic substrates).
- Substrate: Base layer supporting the structure.

The rib confines light laterally via index contrast between the core and cladding, guiding light along its length.

3.2.2. Importance of Rib Waveguides

Rib waveguides are pivotal to advancing photonic technologies due to their structural and functional advantages. Their compact geometry enables the miniaturization of high-performance optoelectronic devices, such as integrated optical circuits and on-chip sensors, by leveraging precise lateral light confinement to reduce device footprint while maintaining low optical losses. These waveguides are highly versatile, compatible with a broad range of materials including silicon, polymers, and III-V semiconductors which allows engineers to tailor optical properties for applications spanning telecommunications, biomedical sensing, and nonlinear optics. Furthermore, their compatibility with scalable, CMOS-compatible fabrication processes ensures cost-effective mass production, making them industrially viable. Beyond practical applications, rib waveguides serve as foundational platforms for exploring fundamental photonic phenomena, such as light-matter interactions and modal behavior, while facilitating the development of novel materials and subwavelength optical systems. These attributes collectively position rib waveguides as indispensable tools for bridging theoretical innovation with real-world photonic device engineering.

3.2.3. Applications

1. **Integrated Optics**: Modulators, lasers, and splitters in PICs and used in silicon photonics for data centers and optical interconnects.
2. **Optical Communication**: Low-loss signal transmission in fiber-optic networks and wavelength-division multiplexing (WDM) components.
3. **Sensing**: Biosensors (detecting refractive index changes in analytes) and environmental sensors (gas detection, temperature monitoring).
4. **Nonlinear Optics**: Enhanced nonlinear effects (e.g., four-wave mixing) due to strong light confinement.
5. **Quantum Photonics**: Guiding single photons in quantum computing circuits.

The large ranges of applications is the most relevant factor that made us chose this type of structure as a case of study.

3.2.4. Advantages of Rib Waveguides

1. **Low Propagation Loss**: Efficient light confinement reduces scattering and bending losses.
2. **Single-Mode Operation**: Easily designed to support single-mode propagation, critical for coherent signal transmission.
3. **Planar Fabrication Compatibility**: Compatible with standard photolithography and etching processes, enabling integration with photonic integrated circuits (PICs).
4. **Thermal Stability**: Robust performance under temperature variations (e.g., silicon-based ribs).
5. **High Integration Density**: Compact design allows dense packing in optical devices.

3.2.5. Disadvantages and Challenges

1. **Fabrication Complexity**: Requires precise etching to maintain rib dimensions (critical for sub-micron waveguides).
2. **Polarization Sensitivity**: May exhibit polarization-dependent losses unless symmetrically designed.
3. **Mode Leakage**: Poorly designed ribs can lead to substrate radiation modes (light leakage into the substrate).
4. **Material Limitations**: Organic/polymer ribs may degrade under high optical power or environmental stress.

3.3. The contrast effect:

In the context of waveguides (particularly optical waveguides) generally refers to the phenomenon where differences in material properties or structural parameters within a waveguide system influence the behavior of propagating waves, such as light or electromagnetic waves. This concept is often tied to how variations in mode confinement affect wave propagation.

3.4. Classification of waveguide by mode structure:

We should consider the classification of waveguides by mode structure as an important factor too, so:

3.4.1. Single-mode waveguide:

A waveguide that supports only one propagation mode, ensuring minimal dispersion and allowing signals to travel long distances with high precision. It's commonly used in fiber-optic communications.

3.4.2. Multi-mode waveguide:

A waveguide that supports multiple propagation modes, allowing different paths for signals but introducing dispersion, which can limit transmission distance. It's often used in short-distance optical communications.

3.5. Software Maple:

Maple is a proprietary computational tool designed for symbolic mathematics, first conceptualized in 1980 by researchers at the University of Waterloo's Symbolic Computation Group. Since the late 1980s, the software has been commercially distributed by Waterloo Maple Inc. (operating as Maplesoft), a technology firm headquartered in Waterloo, Canada. The software's architecture allows users to input equations using conventional mathematical notation and supports custom interface development. It integrates tools for symbolic computation, numerical analysis with high-precision capabilities, and advanced data visualization. Maple also features interoperability with programming languages such as C, Java, MATLAB, and Fortran, as well as integration with applications like Microsoft Excel.

As a comprehensive mathematical platform, Maple merges robust computational algorithms with an intuitive interface to streamline analytical workflows, problem-solving, and graphical representation of data. Key functionalities include:

- **Cross-Disciplinary Problem Solving**: The software addresses challenges across diverse mathematical domains, including calculus, linear algebra, differential equations, statistics, optimization, and financial modeling, while minimizing manual calculation errors.
- **Large-Scale Computation**: It efficiently handles complex or labor-intensive problems that are impractical to solve manually, saving time and effort.
- **Dynamic Visualization**: Users can generate customizable 2D/3D graphs and animations to explore data patterns, theoretical concepts, or solution behaviors.
- **Unified Documentation**: Projects, calculations, visualizations, and annotations can be consolidated into organized, reusable documents for improved workflow transparency.
- **Programming Flexibility**: Maple includes a dedicated scripting language optimized for mathematical operations, enabling concise code development, debugging, and maintenance.
- **Application Development**: With minimal coding expertise, users can design interactive tools for educational, research, or collaborative purposes and distribute them digitally.

The software's latest stable release, version 16, debuted in March 2012, continuing its legacy as a versatile tool for academic, industrial, and research applications.

3.6. The advantages and limitations of the Effective Index Method (EIM)

3.6.1. Advantages of EIM

1. **Computational Efficiency**: Reduces 3D waveguide problems to 2D or 1D approximations, slashing simulation time and resource requirements.
2. **Simplicity**: Easy to implement with basic analytical equations, avoiding complex numerical solvers (e.g., finite-element or finite-difference methods).
3. **Design Intuition**: Provides clear relationships between geometric parameters (e.g., rib width, thickness) and effective indices (neff), aiding rapid prototyping.
4. **Scalability**: Works well for large or thick waveguides ($d>0.8$ μm), where approximations align closely with rigorous methods.

5. **Low-Cost Tool**: Requires no specialized software, making it accessible for preliminary designs.
6. **Compatibility**: Often used as a first-step validation before transitioning to computationally heavy methods.

3.6.2. Limitations of EIM

1. **Accuracy Trade-offs**: Struggles with high-index-contrast or non-rectangular waveguide geometries, leading to errors in n_{eff} calculations.
2. **Polarization Sensitivity**: Assumes separable transverse electric (TE) and transverse magnetic (TM) modes, neglecting polarization coupling in asymmetric structures.
3. **Boundary Effects**: Overlooks field discontinuities at sharp rib edges, underestimating modal losses in tightly confined waveguides.
4. **Multimode Limitations**: Poor at predicting higher-order modes, limiting utility for multimode waveguide analysis.
5. **Material Anisotropy**: Fails to account for anisotropic materials (e.g., crystals or liquid crystals), which require full-vectorial treatments.
6. **Wavelength Sensitivity**: Accuracy degrades at shorter wavelengths (e.g., visible light) where modal fields vary rapidly.

There's something almost elegant about the Effective Index Method (EIM) like finding a shortcut through a labyrinth without losing your way. It's the pragmatic workhorse of waveguide modeling, trading the exhaustive complexity of full 3D simulations for a streamlined, two-step approximation that somehow still gets you where you need to go, slicing through computational overhead like a hot knife through butter. Sure, it glosses over some nuances those whispering higher-order modes or sharp boundary effects but when time is tight and resources lean, EIM bends the rules just enough to deliver the right answers. For thick waveguides, where precision isn't sacrificed at the altar of speed, it's almost poetic: a rough sketch that still captures the soul of the structure. Engineers swear by it during early design sprints, and rightly so why wrestle with finite-element meshes when EIM hands you 80% of the truth in 20% of the time? That's precisely why we chose it as our compass in this work to strike the perfect balance between intuition and rigor, proving that sometimes the smartest tool isn't the heaviest, but the one that lights the way forward.

In this chapter we would:

- Validate TE/TM mode calculation accuracy against structures from Liao (2015) and Thander (2017).
- Compare Effective Index Method (EIM) results for GaAs/GaAlAs waveguides against:
  - Variational EIM + Perturbation Method (VEI+PM)
  - Finite-Difference (FD)
  - Finite-Element (FE) methods.
- Quantify deviations ($|\Delta n|$) for TE_{00}/TM_{00} modes across core heights (*d* = 0.5–0.9 μm).
- Test EIM on GeSi structures (S1/S2/S3) against Thander's numerical methods (HOC-FDM, FFM, BPM, VPM).
- Evaluate confinement efficiency in two structures:
  - *S1*: Low contrast ($|\Delta n| = 0.09$, GaAs/GeSi)
  - *S2*: High contrast ($|\Delta n| = 2.44$, GaAs/Air).
- Calculate total confinement: Γ_2 (82.27%) > Γ_1 (75.95%).
- Map E-field profiles in slab, rib, and lateral regions (Fig. 3.2).
- Generate 3D field intensity plot confirming optical confinement (Fig. 3.3).
- **Parametric Sweep**
  - Vary rib thickness (D = 0.01–0.4 μm) and width (W = 0.1–0.5 μm) for Si/SiO_2 waveguides.
- **Single-Mode Identification**
  - Determine operational bounds:
    - $D < 0.25$ μm (Fig. 3.2)
    - $W < 0.42$ μm (Fig. 3.3).
- **Confinement Efficiency Quantification**
  - Achieved +35.74% confinement gain by increasing height ($H = 0.1 \rightarrow 0.22$ μm, fixed W).
  - Achieved +44.98% confinement gain by increasing width ($W = 0.2 \rightarrow 0.4$ μm, fixed H).
- Simulate TE/TM modes in IPC-E/PSU/NOA72 waveguides with W = 6–10 μm.

- **Spectral Optimization**

3.7. Validation of program:

We start with the validation of TE and TM modes programs to have certain accuracy in obtained results, and as a sample of calculation we used the structures proposed by Liao (2015) and Thander (2017) [20] [21].

The modes of optical rib waveguide are TE_{pq} and TM_{pq}.here p is the number of zero points in lateral and q the number of zero points in vertical, respectively.

In an optical rib waveguide, the modes are classified as TE_{pq} and TM_{pq}, where:

- **p** is the number of interior zero points (nodes) in the field distribution along the **lateral direction (x)**,
- **q** is the number of interior zero points (nodes) along the **vertical direction (y)**.

For the **TE polarization**, the modes $\mathbf{TE_{00}}$, $\mathbf{TE_{01}}$, and $\mathbf{TE_{10}}$ are defined as follows:

- $\mathbf{TE_{00}}$ **Mode**:
  - **p = 0**: No interior nodes in the lateral (x) direction.
  - **q = 0**: No interior nodes in the vertical (y) direction.
  - **Field Distribution**:
    - The electric field is maximum at the center and decays smoothly toward the boundaries.
    - Resembles a bell-shaped curve in both x and y (fundamental mode).

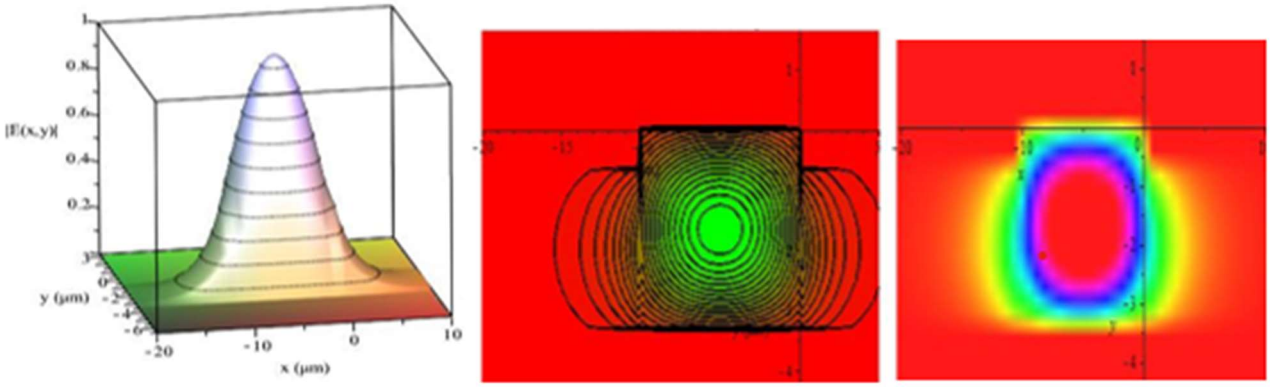

Figure 3.1: *3D plot, contour plot and intensity plot of TE_{00} mode.*

  - **p = 0**: No interior nodes in the lateral (x) direction.
  - **q = 1**: One interior node in the vertical (y) direction.
  - **Field Distribution**:
    - Uniform in x (no variation), but has one zero-crossing in y.
    - Field is "odd" in y (symmetric in x).

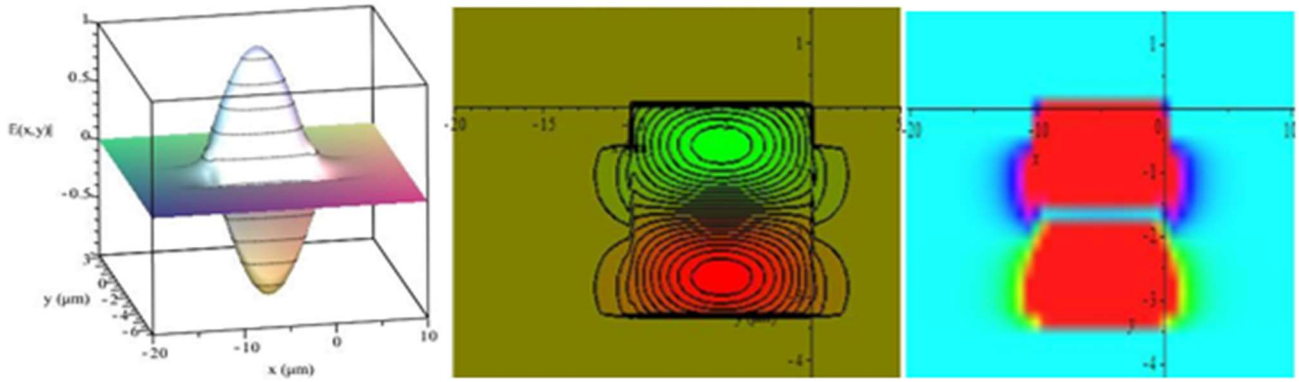

Figure 3.2: *3D plot, contour plot and intensity plot of TE_{01} mode.*

- **TE_{10} Mode**:
  - **p = 1**: One interior node in the lateral (x) direction.
  - **q = 0**: No interior nodes in the vertical (y) direction.
  - **Field Distribution**:
    - Uniform in y (no variation), but has one zero-crossing in x.
    - Field is "odd" in x (symmetric in y).

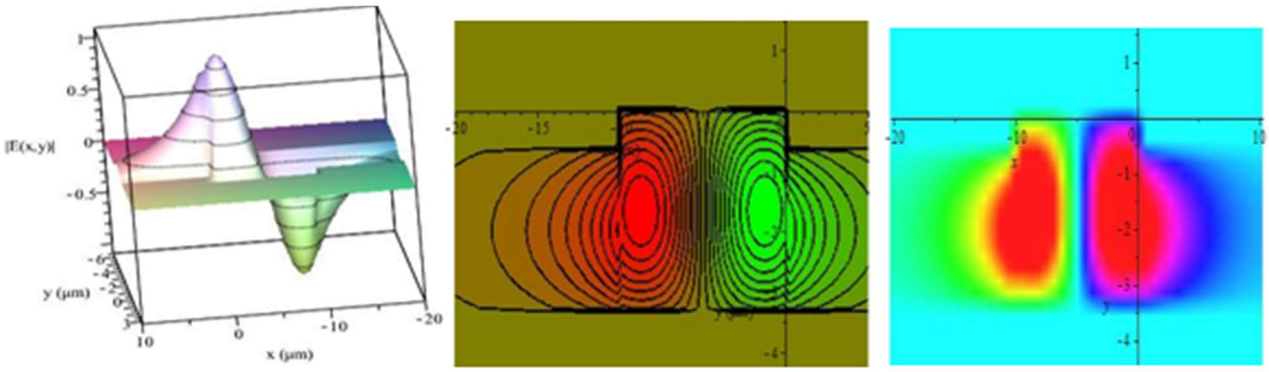

Figure 3.3 : *3D plot, contour plot and intensity plot of TE_{10} mode.*

In order to confirm the proposed program is valid in precision, the results obtained from EIM when analyzing the rib waveguide fabricated by GaAs/GaAlAs [20]are compared with the ones obtained from numerical method from Liao we would take a structure of optic rib waveguide with the following parameters:

RIB GUIDE STRUCTURE	n_{core}	n_s	n_{clad}	*D (µm)*	*d (µm)*	*W (µm)*	*λ (µm)*
ST	*3.44*	*3.40*	*1.0*	*1.0*	*varying*	*3.0*	*1.15*

Table3.1:Parameters for an optical rib waveguide structure.

Where the structure is presented above:

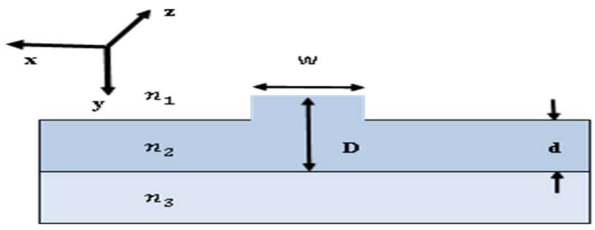

Figure3.4: Structure of optical rib waveguide.

Where, D is the height of the rib area, d is the height of core layer and w is the rib width.

3.6.1. Structure [20]:

- **Core Layer**:
  - **Material**: IPC-E (20 wt%)/PSU electro-optic polymer.
  - **Refractive Indices**:
    - TE modes: n_{core}=1.6608
    - TM modes: n_{core}=1.6563
  - **Height**:
    - Total core height: D=3.3µm (rib region).
    - Slab region height: d=2.65µm (sides of the rib).
- **Cladding Layers**:
  - **Cladding**: NOA72 (UV-curable epoxy).
    - TE: $n_{\textbf{cladding}}$: =1.5406
    - TM: $n_{\textbf{cladding}}$ =1.5404
  - **Substrate** UV61 (UV-curable epoxy).
    - $n_{substreate}$r=1.5472 (same for TE/TM).
- **Rib Width**: w=5–10µm (varied in simulations).

Tables (3.2) and (3.3) represent a comparison between the variational effective index method combined with the perturbation method (VEI+PM), the semi-vectorial finite difference (FD) and vector finite element (FE) methods for both TE_{00} and TM_{00}.

d (μm)	n_{eff} (EIM)	n_{eff} (VEI+PM)	Difference$\|\Delta n\|$	n_{eff} (FD)	Difference$\|\Delta n\|$	n_{eff} (FE)	Difference$\|\Delta n\|$
0.5	3.41426229	3.4138	0.00046229	3.4131	0.00116229	3.4132	0.00106229
0.6	3.414386364	3.4135	0.000886364	3.4136	0.000786364	3.4136	0.000786364
0.7	3.414652748	3.4141	0.000552748	3.4142	0.000452748	3.4141	0.000552748
0.8	3.415054261	3.4147	0.000354261	3.4148	0.000254261	3.4148	0.000254261
0.9	3.41569012	3.4157	9.88E-06	3.4157	9.88E-06	3.4156	9.012E-05

Table3.2: Effective indices calculated using the effective index method (EIM) for the TE_{00} mode.

d (μm)	n_{eff} (EIM)	n_{eff} (VEI+PM)	Difference	n_{eff} (FD)	Difference
0.6	3.412708565	3.4123	0.000408565	3.4119	0.000808565
0.7	3.41292938	3.4126	0.00032938	3.4124	0.00052938
0.8	3.413308656	3.4131	0.000208656	3.413	0.000308656
0.9	3.413938015	3.4138	0.000138015	3.4138	0.000138015

Table 3.3: Effective indices calculated using the effective index method for the TM_{00} mode.

The Effective Index Method (EIM) proves to be a reliable tool for calculating the effective refractive indices of a GaAs/GaAlAs rib waveguides. Its results align remarkably well with those obtained from more complex techniques like the Variational Eigenmode with Perturbation Method (VEI+PM), Finite-Difference (FD), and Finite-Element (FE) methods, as well as with previous findings by Liao et al. (2015).

As the height of core layer (d) increases from 0.5 μm to 0.9 μm, the differences between EIM and these numerical methods shrink significantly. For example, at d = 0.5 μm, the deviation between EIM and VEI+PM was 0.00046, but this dropped to a mere -9.88 x 10^{-6} at d = 0.9 μm, showing near-perfect convergence for thicker waveguides. Similarly, the FD and FE methods consistently exhibited deviations below 0.00116 across all thicknesses, with minimal differences (less than 0.00025) when d was between 0.8 μm and 0.9 μm.

These findings support Liao et al.'s (2015) conclusions: EIM achieves high accuracy when waveguide dimensions exceed 0.8 μm, a crucial range for optimizing a GaAs/GaAlAs rib waveguides. The small discrepancies at smaller 'd' values (like 0.00046 at d = 0.5 μm) are consistent with the inherent approximations of EIM, particularly how it handles modal field boundaries, as noted in earlier research.

Nevertheless, the strong agreement between EIM and rigorous numerical methods for larger 'd' values confirms EIM's suitability for rapidly and efficiently designing optical rib waveguide.This consistency with established theoretical and experimental frameworks (Liao et al., 2015) underscores the reliability of these results and solidifies EIM's value as a practical tool for engineering applications.

Considering the famous geometrical structure parameters of GaAs and GeSi [21] rib waveguides that follow in our second part of validation and make comparison between EIM obtained results and Thander values.

Structure	n_core GaAs	n_s GeSi	n_clad Air	D (µm)	d (µm)	W (µm)	λ (µm)
S1	3.44	3.34	1	1.3	0.2	2	1.55
S2	3.44	3.36	1	1	0.9	3	1.55
S3	3.44	3.435	1	6	3.5	4	1.55

Table3.4: Optical and Geometrical structure parameters of GaAs and GeSi rib wave guides.

For Thunder we would take different structures of an optic rib waveguide with the different parameters that follow:

A key distinction of the EIM is the absence of an S1 value, setting it apart from other analytical techniques. However, for the S2 and S3 values**,** there's remarkable consistency across different methods. S2 values typically range from 3.394 to 3.396, and S3 values from 3.43666 to 3.43698, indicating a high degree of agreement and reliability for these specific parameters. S1 values (3.386–3.390) exhibit slightly more variation, highlighting how different methods can have varying sensitivities to certain waveguide characteristics.

	Structures		
Method	**S1**	**S2**	**S3**
EIM	-	3.395479409	3.436980241
HOC-FDM	3.3902787	3.3958327	3.4367243
Stern [22]	3.3869266	3.3953942	3.4366674
FFM [23]	3.3904487	3.3948874	3.4367238
FDM [23]	3.3906186	3.3951678	3.4368423
FDM [23]	3.3901687	3.3954802	3.4367068
BPM [23]	3.3902687	3.3944707	3.4368358
VPM [23]	3.3905686	3.3950156	3.4367468

Table3.5: Comparison of Effective indices values for GaAs Geometries Using Different Methods.

The absence of EIM data for S1 likely stems from the structure's violation of EIM's core assumptions (e.g., subwavelength features or high anisotropy), rendering the method invalidconsistent with EIM's known limitations for complex photonic topologies.

3.8. Contrast effect:

In this part we would like to put on light on the contrast effect for the structures of optic rib waveguides that follow:

Structure	n_core GaAs	n_s GeSi	n_clad	$\|\Delta n\|$ (n_core- n_clad)	D (µm)	d (µm)	W (µm)	λ (µm)
S1	3.44	3.35	3.35(GeSi)	0.09	1.0	0.9	3	1.15
S2	3.44	3.35	1 (Air)	2.44	1.0	0.9	3	1.15

Table3.6: Optical and Geometrical structure parameters of GaAs and GeSi rib wave guides

In a simple definition the contrast is the difference between the core and the cladding refractive indexes and its influence on the confinement of a guide.

From figure (3.5), we can see the influence of the contrast on the vertical and the lateral confinement, in which S2 has the bigger contrast logically has bigger confinement in both directions (x and y).

The confinement have a positive correlation, since they move in the same direction; The greater $|\Delta n|$ is, the better the confinement.

The total confinement in S2 is greater than the total confinement of S1, in which:

(Γ_2 =82.27089261% > Γ_1= 75.94942558%).

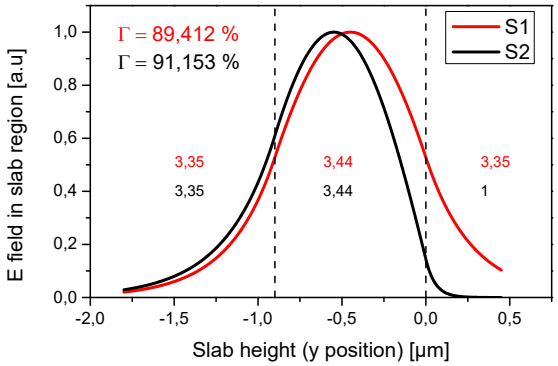

(a) E field in slab region

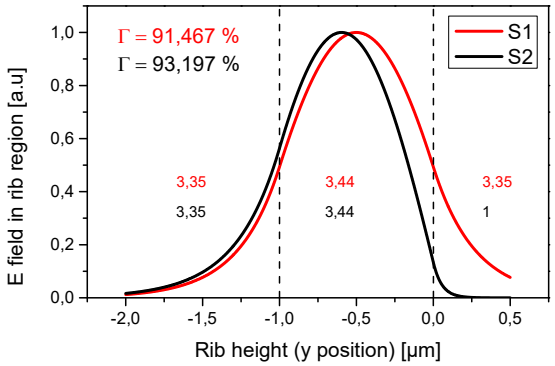

(b) E field in rib region

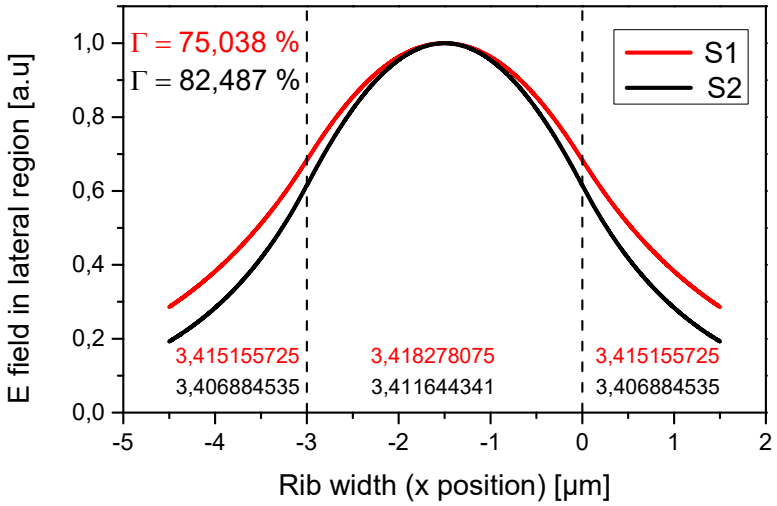

(c) E field in lateral region

Figure3.5: E field distribution where (a) E field in slab region, (b) E field in rib region and (b) E field in lateral region.

Here is a 3D plot of field intensity in the chosen structure previously for an optic rib waveguide by knowing that x is the rib width and y is the height of the rib area:

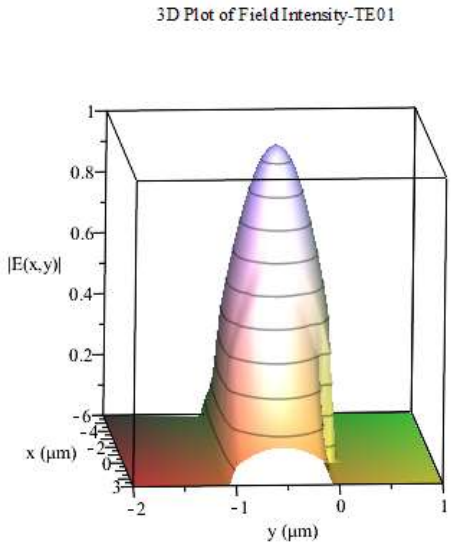

Figure3.6:3D plot of field intensity for the second structure.

The field intensity rapidly drops to very low values as x and y move away from the central peak (towards the "flat" regions at the base of the plot). This demonstrates optical confinement**,** where the light is largely contained within the higher refractive index core of the waveguide, and only an evanescent field extends into the surrounding lower refractive index cladding and substrate.

The plot shows a clear, bell-shaped peak in the field intensity, centered around x ≈ 0 and y ≈ -0.5 to 0 µm. This indicates the region where the light is most strongly confined and propagates.

Along the y-axis, the field exhibits a shape resembling a Gaussian or parabolic profile, which is typical for guided modes in optical waveguides. It peaks near the center and decays rapidly away from it. The "01" mode typically implies a single lobe in the y-direction, which is consistent with the plot.

We did not put the 3D plot of field intensity for the first structure since there is no big difference between them and that would not be appearing clearly on the curves.

3.9. Optimisation of a single-mode rectangular rib waveguide:

In this section we would change two essential parameters (the height and the width) of an optic rib waveguide structure in order to optimize it for obtaining enhanced confinement for a single-mode guide.

And we should considerate that the dominant geometric parameter in rib waveguides is the width of the rib and it controls mode confinement and the guide effective index**.**

And the rib thickness which is the secondary important parameter and becomes vital for polarization-sensitive designs and nonlinear optics

The structure studied for this section is about a Silicon (Si) core and a Silica (SiO2) clad and substrate, it is noticeable that this structure is a symmetric structure.

In this study we would vary two parameters for the same structure; we would vary rib thickness D=[0.01-0.4] μm and waveguide (rib) width w= [0.1-0.5] μm.

The obtained results are represented in the figures (3.7) and (3.8).

RIB GUIDE STRUCTURE	n_{core}	n_s	n_{clad}	*D (µm)*	*d (µm)*	*W (µm)*	*λ (µm)*
ST	*3.47*	*1.44*	*1.44*	*varying*	*1.0*	*varying*	*1.55*

Table3.7: Parameters for an optical rib waveguide structure.

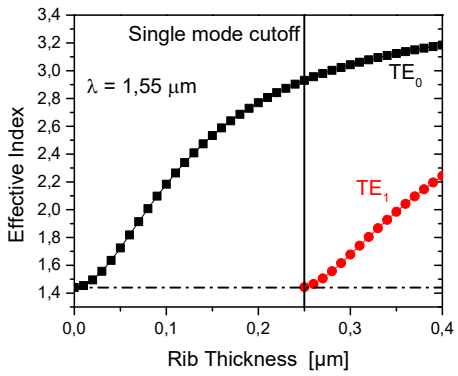

Figure3.7: The variation of the refractive index vs the rib thickness for TE mode.

The region to the left of the "Single mode" line (approximately rib thickness < 0.25 µm) is the single-mode operation region**.**

Operating in the single-mode regime is highly desirable for many applications, especially in optical communications, as it prevents modal dispersion (different modes traveling at different speeds, causing signal distortion) and simplifies device design.

The region to the right of the "Single mode" line (approximately rib thickness > 0.25 µm) is the multi-mode operation region.

In this region, both the fundamental TE_0 mode and the first higher-order TE_1 mode can propagate. As the rib thickness continues to increase, even more higher-order modes (TE_2, TM_0, etc.) would eventually become guided, although they are not shown on this specific plot.

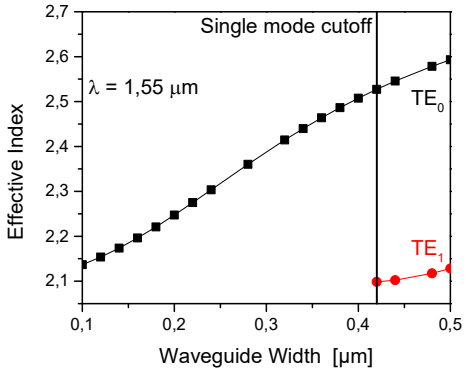

Figure3.8: The variation of the refractive index vs the rib width for TE mode.

The region to the left of the "Single mode" line (approximately waveguide width < 0.42 µm) represents the single-mode operation region**.**

To guaranty a good performance (great confinement) in the optic rib guide we chose two values for each parameter w and D to compare with each other and select the better confinement.

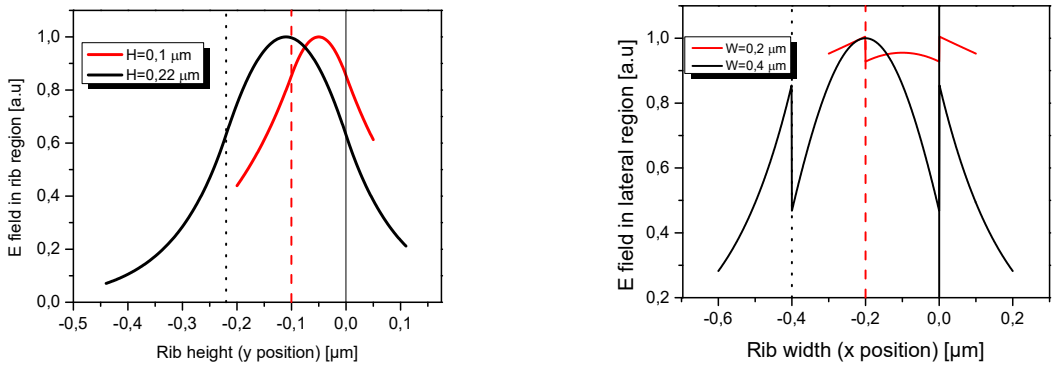

Figure 3.9: Comparative curves describing the influence of parameters on confinement.

The confinement efficiency of the waveguide structure exhibits a strong dependence on its geometric parameters. For a fixed width (*W*), increasing the waveguide height (*H*) from 0.1 µm to 0.22 µm enhances the confinement by approximately 35.74 percentage points (from 45.23%to 80.97%) reflecting improved light-matter interaction. Similarly, for a

fixed height (*H*), increasing the width (*W*) from 0.2 μm to 0.4 μm elevates confinement by 44.98 percentage points (from 34.29% to 79.27%).Notably, the width exerts a more pronounced influence on confinement than the height for this structure, as evidenced by the sharper increase in confinement per unit dimensional change (ΔW=0.2 μm vs. ΔH=0.12 μm). These trends align with theoretical expectations, where larger cross-sectional dimensions enhance the effective refractive index contrast, thereby tightening modal confinement. However, such gains must be balanced against the risk of multimode propagation at larger *W* and *H*, which could introduce intermodal dispersion. This analysis underscores the critical role of dimensional optimization in tailoring waveguide performance for applications prioritizing either single-mode stability or high confinement.

3.10. Analysis of optical rib waveguides based organic/polymer materials:

In recent years, organic/polymer photonic devices have garnered significant attention and emerged as a key area of research within polymer photonics. This interest is primarily driven by the fabrication challenges associated with high-speed active photonic devices, such as electro-optic (EO) modulators and tunable attenuators, based on inorganic optical materials. Compared to inorganic crystalline materials, polymer-based EO materials offer several advantages: low permittivity in the microwave and millimeter-wave range, high EO coefficients, ultrafast response times, and simpler fabrication processes.

An optical waveguide is a fundamental component in organic/polymer photonic devices. Given the physical and chemical characteristics of polymer materials, such waveguides are typically fabricated through spin-coating followed by reactive ion etching. The rib waveguide structure is particularly suitable for these materials. To accurately simulate and predict the performance of polymer photonic devices, it is essential to theoretically analyze and optimize the optical waveguide structure. However, due to the complex geometry of rib waveguides, analytical solutions are generally unattainable, necessitating the use of numerical methods. Common analytical approaches include the finite element method, finite-difference time-domain method, beam propagation method, transfer matrix method, mode-coupling theory, and the effective index method (EIM) [20].

3.10.1. Optimizing rib waveguide width

It is assumed that the electro-optic polymer materials in the waveguide core and rib areas are all equally poled and cladding materials are assumed to be semi-infinite in the following discussions.

In this section we would vary the rib waveguide width (w:6 - 10 μm , Δw =1 μm) where the core is Isophorone diisocyanate-based Polyphosphonate Ester PC-E(20wt%)/PSU where PSU Is the matrix polymer**,** Polysulfone and IPC-E (20wt%) Is a functional additive incorporated at 20% by weight into the PSU matrix and the ultraviolet curable epoxy NOA72 is adopted as upper cladding.

We use polymers for many reasons such as:

- ✓ High thermal stability.
- ✓ Excellent hydrolytic stability (resistance to hot water/steam).
- ✓ Good mechanical properties (toughness, rigidity).
- ✓ Good electrical insulation properties.
- ✓ Inherent flame retardancy.
- ✓ Good chemical resistance (though attacked by some solvents like ketones and chlorinated hydrocarbons)
- ✓ Transparency

Starting the analysis for TE mode:

RIB GUIDE STRUCTURE	n_{core}	n_s	n_{clad}	*D (μm)*	*d (μm)*	*W (μm)*	*λ (μm)*
ST	*1.6608*	*1.5472*	*1.5406*	*3.3*	*2.65*	*varying*	*1.55*

Table 3.8: Parameters for an optical rib waveguide structure for TE mode.

For TM mode:

RIB GUIDE STRUCTURE	n_{core}	n_s	n_{clad}	*D (μm)*	*d (μm)*	*W (μm)*	*λ (μm)*
ST	*1.6563*	*1.5472*	*1.5404*	*3.3*	*2.65*	*varying*	*1.55*

Table3.9: Parameters for an optical rib waveguide structure for TM mode.

It is noticeable that the refractive index differs for TE (Transverse Electric) and TM (Transverse Magnetic) modes in waveguides due to geometric anisotropy and boundary conditions, even in isotropic materials. TE modes (electric field parallel to interfaces) and TM modes (magnetic field parallel, but electric field has a normal component) experience different confinement effects at core-cladding interfaces. This asymmetry causes light to "see" distinct effective refractive indices, a phenomenon called modal birefringence.

The phase constants β [proportional to n_{eff} for TE and TM modes are different due to the distinct boundary conditions [5].Fundamentals of Optical Waveguides (2nd ed.), Academic Press. ISBN: 978-0125250962.).

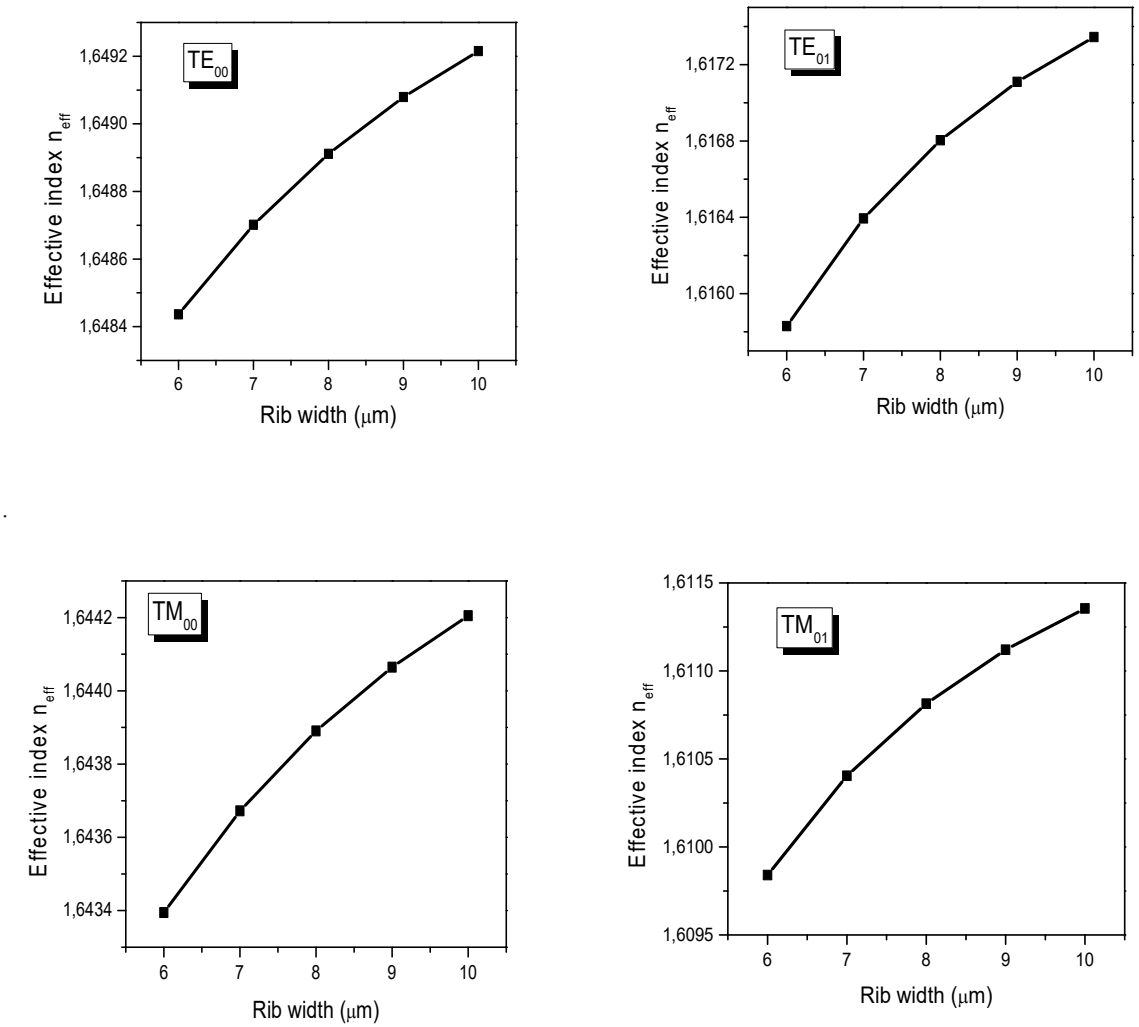

Figure3.10: Effective indices vs. rib width and their polarization modification for TM_{00},TE_{00},TM_{01},TE_{01}

The curves clearly show that as the rib width of the waveguide increases, the effective refractive index (n_{eff}) for the modes also increases. wider waveguides generally support modes with higher effective indices. The effective index represents the phase velocity of the light propagating in the waveguide, effectively acting as the refractive index for the guided mode.

The effective refractive index is directly related to the confinement of the optical mode within the waveguide core. A higher effective index (approaching the refractive index of the core material) indicates stronger confinement of light within the high-index core region. Conversely, a lower effective index (closer to the cladding index) means the light is less confined and more of its energy extends into the lower-index cladding. [5]

The lateral and the total confinement of intensity in the rib waveguide for TE and TM polarizations of the fundamental mode a function of the waveguide width are shown in Figure (3.11):

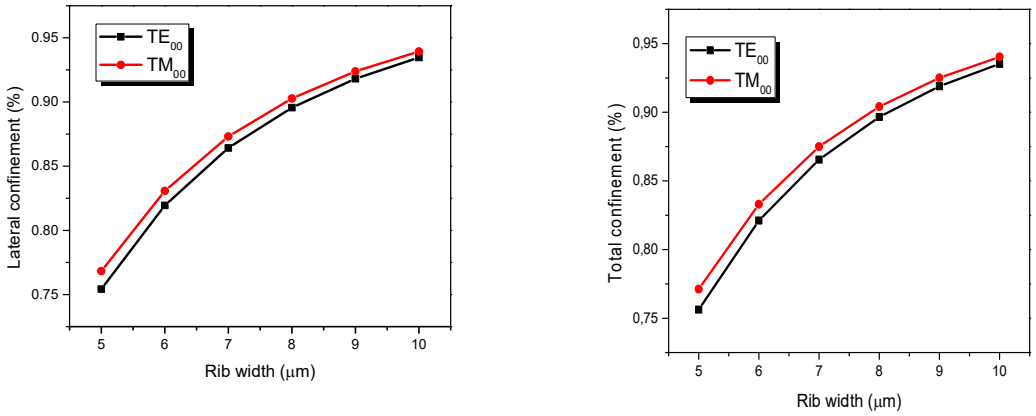

Figure3.11: Comparative curves that show the difference between lateral and total confinements for fundamental mode.

It can be noted that the confinement increases with increase in core width. The TM mode appears to be better confined in the central part of the rib waveguide. [24] [25]

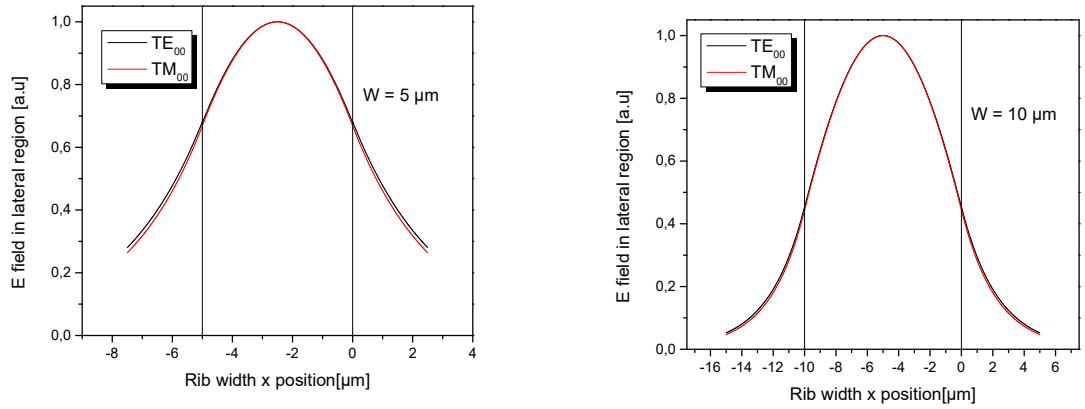

Figure3.12: Comparative curves that show present the lateral field intensity in the rib waveguide for TE and TM polarizations for two different width value.

It is also worth noting in passing that the mode profiles presented above are normalized to have unity peak intensity. This has been done so that a direct comparison can be direct comparison can be made. It is more usual to normalize these profiles to unity power flow, but in general this results in different amplitudes flow, when plotting both profiles on the same axis, and hence visual comparison is more difficult. If we plot both the TE and the TM phase change on reflection for the TM mode is always greater than that for the TE mode.

From figure (3.7) it is also clear that as the waveguide is increased in size from 5 to 10 µm, the TE and TM modes increased in size, the TE and TM modes become similar, and the polarization become similar, and the polarization dependence is reduced. Therefore, increasing

the waveguide thickness brings the TE and TM modes closer together in terms of their field profiles. However, there is still a finite separation between the degree of confinement, although in practice the difference may be negligible for some applications. The TE field slightly expands in the thinner active region, and this effect is more important as the refractive index is reduced. Increasing the refractive index yields more similar field profiles of the TE and TM modes in the waveguide. [24]

3.10.2. Spectral optimization

Supposing the center wavelength of a semiconductor laser is 1550nm and the span of center wavelength considered here is ±20nm, which is reasonable for example the center wavelength tolerance of laser diode module (Newport's LPM1550-05E) is ±20nm. Because of the narrow span of the center wavelength, the material dispersion can be ignored here and only mode dispersion needs to be concerned. The curves of effective index vs. wave length for TM, TE modes are plotted in Figure (3.8) (D=3.3 μ m, d =2.65 μ m, w= 6 μm , λ=1530-1570nm).As shown in Figure (3.8), the differences of effective index obtained by these methods are similar numerically to the curves in Figure (3.5) for TM, TE modes and the effective index decreases with the increase of operating wavelength.

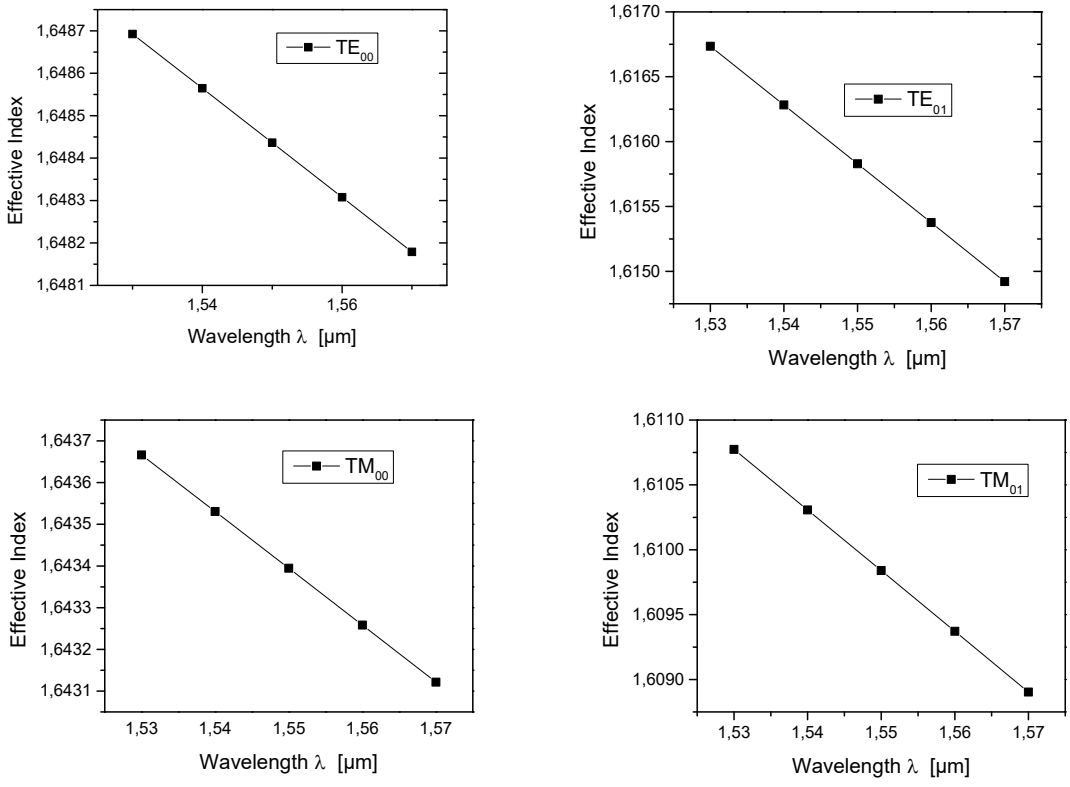

Figure3.13: Effective indices vs. operating wavelength and their polarization modification for TM_{00},TE_{00},TM_{01},TE_{01}.

The curves illustrate a linear decrease in the effective index of the modes as the wavelength increases from 1.53 μm to 1.57 μm. This behavior is indicative of dispersion within the optical waveguide and provides important information for understanding and designing optical devices operating in this wavelength range.

For instance, in silicon photonics, wavelength-dependent optimization might involve selecting the near-infrared C-band (∼1550nm) to minimize propagation loss while ensuring high confinement. In nonlinear waveguides, phase-matching at specific wavelengths is critical for efficient frequency conversion processes.

3.11. Conclusion

In summary, this analysis of optical rib waveguides underscores the high accuracy of the Effective Index Method (EIM) for GaAs/GaAlAs structures, particularly for core heights exceeding 0.8 μm, positioning it as a reliable tool for practical design. The study unequivocally demonstrates that refractive index contrast is a primary driver of optical confinement, with high-contrast waveguides exhibiting significantly tighter mode confinement compared to their low-contrast counterparts. For Si/SiO_2 waveguides, critical dimensional limits for single-mode operation were established, highlighting the dominance of waveguide width as a geometric parameter for enhancing confinement, albeit with potential multimode propagation risks. Polarization dependence was observed, with TM modes generally more centrally confined, though this sensitivity diminishes at larger waveguide widths. Spectral analysis revealed a linear relationship between effective index and wavelength, indicating modal dispersion and enabling wavelength-selective optimization. Furthermore, the performance of polymer waveguides, specifically IPC-E/PSU core with NOA72 cladding, showed predictable scaling of effective index with width and birefringence consistent with theoretical models. These findings align with existing benchmarks and theoretical frameworks, providing robust guidelines for the design and optimization of optical rib waveguides for various applications, emphasizing the trade-offs between confinement, single-mode operation, polarization sensitivity, and material choices.

General conclusion

This study has explored the theoretical foundations and practical implementation of the Effective Index Method (EIM) in the analysis of optical rib waveguides. Beginning with a broad overview of waveguide physics and photonics, we established the importance of confinement, geometry, and material choices in designing efficient optical structures.

We then delved into planar and slab waveguide models, using Maxwell's equations to derive guided mode behavior, particularly for TE and TM modes. The EIM was introduced as a powerful, semi-analytical approach to reduce complex 2D and 3D waveguide problems into manageable 1D models.

Applying the EIM to rib waveguides, we demonstrated how this method allows rapid yet reliable analysis of mode propagation, effective refractive indices, and confinement properties. The study highlighted the benefits of rib structures in integrated optics, particularly for their balance between performance, fabrication ease, and single-mode operation.

Through validation with existing analytical and numerical results, the EIM proved to be a practical tool for early-stage design and optimization. We used the Maple software to simulate various configurations, revealing how changes in rib width, core height, and refractive index contrast affect mode confinement.

Despite some limitations such as complex geometries the EIM remains a highly effective method for waveguide design. Its strength lies in simplifying complex calculations while maintaining acceptable precision.

Ultimately, this thesis confirms that EIM is an indispensable technique in photonic device modeling, offering the speed, clarity, and design intuition needed to advance integrated photonics. It serves as a bridge between rigorous computation and real-world engineering, guiding the design of next-generation optical circuits.

Future Perspective

Quantum-Enhanced Photonic Integration

Building on this demonstrated expertise in high-confinement waveguide design, this work lays the foundation for next-generation quantum photonic circuits. This optimization of TM-mode confinement (5–7% enhancement in polymer waveguides) and precise spectral control (1530–1570 nm dispersion characterization) directly address two critical challenges in quantum light manipulation:

- Scalable photon sources:

High-index-contrast GaAs/Air structures ($|\Delta n|=2.44$, 82.27% confinement) could host quantum dot emitters, leveraging your single-mode dimensional thresholds ($W<0.42$ μm) to generate indistinguishable photons.

- Noise-resilient interconnects:

Obtained polarization management strategies (birefringence suppression at $W>8$ μm) enable topologically robust waveguide arrays suppressing backscattering in entangled photon routing.

Optical Neural Acceleration via Programmable Waveguides

Building on the confinement scaling principles (+44.98% with width optimization in Si/SiO_2 waveguides), this work pioneers ultra-efficient neuromorphic photonics.Our dimensional thresholds for single-mode operation ($W<0.42$ μm) and spectral characterization (1530–1570 nm dispersion) directly enable two revolutionary capabilities:

1. **Optical "Neurons":**
    - Design reconfigurable waveguide meshes using thermo-optic phase shifters trained via ML (Machine Learning) algorithms.
    - *Mechanism*: Confinement scaling emulates synaptic weighting – wider waveguides (0.2→0.4 μm) boost optical "signal strength" akin to biological neural amplification.
2. **Wavelength-Division Multiplexing (WDM)**:
    - Leverage the linear effective index-wavelength relationship (Fig. 3.8) to implement parallel optical data channels.

Bibliography

[1] O. Darrigol, Electrodynamics from Ampère to Einstein., Oxford University Press., (2000). .

[2] D. Marcuse, Theory of Dielectric Optical Waveguides (2nd ed.)., Academic Press., (1991). .

[3] D. M. Pozar, Microwave Engineering (4th ed.)., Wiley., (2011). .

[4] R. E. Collin, Field Theory of Guided Waves (2nd ed.)., . Wiley-IEEE Press., (2000). .

[5] K. Okamoto, Fundamentals of Optical Waveguides (3rd ed.)., . Academic Press., (2021)..

[6] A. W. &. L. J. D. Snyder, Optical Waveguide Theory., Springer.v, (1983). .

[7] A. B. Buckman, Guided-Wave Photonics., Saunders College Publishing., (1992). .

[8] H. H. M. &. S. T. Nishihara, Optical Integrated Circuits., McGraw-Hill, (1989)..

[9] C. C. e. a. Lee, Polymer Waveguides: Fabrication and Applications. Progress in Quantum Electronics,, (2018)., pp. 57, 1-34..

[10] G. T. &. K. A. P. Reed, Silicon Photonics: An Introduction., Wiley., (2004)..

[11] E. Hecht, Optics (5th ed.)., Pearson., (2017). .

[12] M. &. W. E. Born, Principles of Optics: Electromagnetic Theory of Propagation,, (1999). .

[13] F. L. P. L. M. &. P. L. S. Pedrotti, Introduction to Optics (3rd ed.)., Cambridge, (2017). .

[14] A. &. Y. P. Yariv, Photonics: Optical Electronics in Modern Communications (6th ed.)., Oxford University Press., (2007). .

[15] B. E. A. &. T. M. C. Saleh, Fundamentals of Photonics (3rd ed.)., Wiley.v, (2019). .

[16] A. H. S. C. &. P.-M. M. Taflove, Taflove, A., Hagness, S Computational Electrodynamics: The Finite-Difference Time-Domain Method (5th ed.)., . Artech House., (2022). .

[17] R. M. &. T. P. P. Knox, " Integrated Circuits for the Millimeter through Optical Frequency Range. Proceedings of the MRI Symposium on Submillimeter Waves,," p. 497–516., (1970). .

[18] R. A. &. L. J. P. Soref, "[ARTICLE] Soref, Single-Crystal Silicon: A New Material for 1.3-1.6 µm Integrated Optics. Optical Engineering,," p. 1186–1192., (1986). .

[19] S. P. e. a. Pogossian, " The Single-Mode Condition for Silicon Rib Waveguides.," p. 1851–1853., (1998). .

[20] K. e. a. Liao, "Mode Confinement in High-Index-Contrast Waveguides.," p. 1–11., (2015). .

[21] M. &. S. E. Thander, "Comparative Analysis of Optical Waveguide Structures.," *Optik, 131, ,* p. 1034–1042., (2017). .

[22] M. S. Stern, " Finite difference analysis of planar optical waveguides.," *Progress in Electromagnetics Research, ,* p. 123–186., (1995). .

[23] W. &. H. H. A. Huang, " A simple variational approach to optical rib waveguides.," *Journal of Lightwave Technology, ,* p. 56–61., (1991). .

[24] Abdesselam Hocini, Ahmed Bouchelaghem, Djamel Saigaa, Mounir Bouras, Touraya Boumaza, Mohamed Bouchemat, Birefringence properties of magneto-optic rib waveguide as a function of refractive index, J Comput Electron 12 (2013) 50–55

[25] Vivien, L., Laval, S., Dumont, B., Lardenois, S., Koster, A., Cassan, E.: Polarization-independent single-mode rib waveguides on silicon-on insulator for telecommunication wavelengths. Opt. Commun. 210 (2002) 43–49

الجمهورية الجزائرية الديموقراطية الشعبية
وزارة التعليم العالي والبحث العلمي

جامعة عبد الحميد بن باديس-مستغانم-
كلية العلوم الاجتماعية و الإنسانية

تصريح شرفي خاص بالالتزام بقواعد النزاهة العلمية لإنجاز البحث

أنا الممضية أدناه،

الطالبة:شمومة اميرة خيرة رقم التسجيل الجامعي :191937038710

الحاملة لبطاقة التعريف الوطنية رقم: 110010970006910003

والصادرة بتاريخ: 2024/07/21

عن سور-مستغانم

المسجلة بـ**كلية العلوم الدقيقة والإعلام الآلي / قسم علوم المادة**

شعبة فزياء / التخصص فزياء المواد

والمكلف بإنجاز مذكرة ماستر بعنوان:

طريقة معامل الانكسار الفعال وتطبيقها على دليل الموجة الضوئي الشريطي

أصرح بشرفي أني ألتزم بمراعاة المعايير العلمية والمنهجية ومعايير الأخلاقيات العلمية والنزاهة الأكاديمية المطلوبة في إنجاز البحث ، وأتحمل المسؤولية الشخصية عن كل المحتوى المتضمن في البحث المذكور أعلاه .

التاريخ: 22/06/2025

إمضاء المعنية

Ch.

* ملحق القرار الوزاري رقم 933 المؤرخ في 28 جويلية 2016 الذي يحدد القواعد المتعلقة بالوقاية من السرقة العلمية ومكافحتها.